UNIVERSITY OF CALIFORNIA
SANTA CRUZ

Cortical-Thalamic Axons are Required for Retinal Ganglion Cell Targeting to the Mouse Dorsal Lateral Geniculate Nucleus

A dissertation submitted in partial satisfaction
of the requirements for the degree of

DOCTOR OF PHILOSOPHY

in

Molecular, Cell and Developmental Biology

by

James A. Shanks

December 2015

The Dissertation of James A. Shanks
is approved:

_____
Professor David Feldheim, Ph.D.

_____
Professor Alan Zahler, Ph.D.

_____
Professor Bin Chen, Ph.D.

_____
Tyrus Miller
Vice Provost and Dean of Graduate Studies

Table of Contents

List of Figures v

Abstract vii

Acknowledgements x

Chapter 1 1

Structure of the retina 3

Retinal ganglion cells and parallel circuits 5

Timing of retinothalamic circuit formation 5

Disruption of eye specific domains in dLGN 6

RGC axon targets and associated behaviors 7

Molecules necessary for RGC axon targeting in the visual system 12

Mouse visual system receives cortical input 13

Summary 17

Chapter 2

Methods

Transgenic mice 19

Tracing RGC axons 20

Immunohistochemistry 20

Histochemistry 21

In situ RNA hybridization 22

Silicon probe in-vivo electrophysiology 23

Fear Conditioning 27

Cued Swim Maze 27

Pupillary light response 28

Locomotor activity 29

Chapter 3: Investigating the necessity of cortical inputs during development of the mouse visual system

Introduction 30

Results 33

Discussion 49

Conclusions 54

Cortical layer 6 necessary for proper RGC axon targeting to dLGN

Bibliography 56

List of Figures

1	Simplified schematic of the retina	4
2	Defects in eye specific layer location and incomplete refinement of RGC axons in the dLGN	7
3	Sagittal view of the mouse visual system	10
4	dLGN and SC can be separated into distinct layers that receive input from different types of RGCs	11
5	Cortical circuitry of mouse visual system	14
6	Timing of layer 6 cortical innervation within the dLGN	16
7	Schematic of the mouse visual system including descending and ascending cortical projections	18
8	Emx1-Cre;Tra2β mutant mice have severe cortical tissue loss and loss of RGC inputs to the dLGN	35
9	Image forming RGCs fail to properly target the dLGN	36
10	Tra2β cKO LGN tissue is similar to that of wild type controls	38
11	Tra2β cKO retinas have normal RGC populations and distributions	39
12	Image forming RGCs fail to properly target the dLGN of Tbr1 KO animals	40

13 Significant changes were observed in flashing spot and white noise responses, but not in direction and orientation selectivity 42

14 Pupillary light reflex and circadian rhythms are normal in Tra2β cKO animals

15 Tra2β cKO animals perceive light and can navigate a complex task 48

16 A proposed model of my work: Cortical layer 6 neurons provide a membrane bound or secreted molecule, or an activity, for the proper targeting of RGCs to the dLGN 57

Abstract

Cortical-Thalamic Axons are Required for Retinal Ganglion Cell Targeting to the Mouse Dorsal Lateral Geniculate Nucleus

by

James A Shanks

The human brain contains over 85 billion neurons, which make trillions of synapses in a very ordered and stereotypical manner (Williams and Herrup, 1988). The human cerebral cortex, which contains over 20 percent of the total number of neurons within the brain, is responsible for critical functions such as memory, attention, perception, awareness, language, thought, and consciousness, and it dedicates over 30 percent of the total area to the process of vision, 8 percent for touch, and 3 percent for hearing (Grady et al., 1993). One major question in the field of neuroscience is: how do neurons navigate the extremely complex environment of the developing brain that contains an endless amount of possible synaptic partners and continually, precisely, and stereotypically find their appropriate synaptic targets?

Many disorders that affect the human population can be attributed to the loss of the precise wiring within the brain, including mental retardation, schizophrenia,

and autism (Tye and Bolton, 2013; Kana et al., 2011; Huttenlocker, 1991; Buchmann et al., 2014). Recent studies that utilized fMRI to investigate brain activity in people who suffer from schizophrenia, a disorder that renders the inflicted an inability to perceive what is real, show a distinct loss of cortical activity in the visual thalamus resulting from a loss of thalamo-cortical circuitry. Elucidating the mechanisms responsible for the proper wiring of the brain is of paramount importance, and could lead to possible remedies for afflictions such as schizophrenia.

The mouse visual system has become an increasingly popular model to study the development of neural circuits given the vast genetic tools and the ease with which the output neurons of the retina, retinal ganglion cells (RGCs), can be labeled. Multiple distinct targets of RGCs have been well characterized and many behaviors are associated with these nuclei that can be easily assayed to detect for dysfunction (Sweeney et al., 2014; Osterhout et al., 2015). It has been demonstrated that activity is necessary for the refinement of RGCs in the dLGN during development and the proper placement of RGCs within eye specific domains is reliant on specific receptor tyrosine kinases (Rossi et al., 1988; Pfeifenberger et al., 2005). Mounting evidence suggests that specific transmembrane adhesion molecules are necessary for the proper targeting of RGCs to specific visual nuclei responsible for multiple non-image forming behaviors, including circadian rhythms, the pupillary light reflex, and image stabilization (Osterhout et al., 2011; Osterhout et al., 2015; Sun et al., 2015; Su et al., 2011). Molecules necessary for the proper targeting of image forming nuclei

including the dLGN and the superior colliculus (SC), a midbrain target necessary for reflexive head and eye movements, remain elusive.

While the retina sends projections to specific subcortical nuclei, many of these same nuclei also receive cortical input from either layer 5 or layer 6 of the visual cortex (V1). The timing and patterns of innervation of cortical layer 6 neurons in the dLGN has recently been elucidated (Seabrook et al., 2013). These data indicate that the removal of RGC axons from the dLGN during development allows cortical neurons to innervate the dLGN at earlier time points, suggesting RGC axons control the timing of innervation. Whether cortical neurons affect the innervation patterns of RGCs is not well understood.

In order to better understand the role of V1 input during the development of the mouse visual system, I utilized a transgenic mouse harboring a floxed conditional allele for a splicing factor that when removed with a cre-recombinase driver line, only expressed in cortical tissue, results in the almost complete loss of the mouse neo-cortex. Surprisingly, the animal is viable and thus allowed me to investigate the necessity of V1 innervation during the development of the mouse visual system including innervation patterns of RGCs within multiple subcortical nuclei. I was also able to investigate well known non-image forming behaviors, including the pupillary light reflex, to test for the necessity of cortical layer 5 input, and circadian rhythms to better understand if the cortex modulates sleep wake cycles. Also, I tested whether mice lacking cortical input and almost complete loss of RGC inputs to the dLGN can

perceive light and whether this perception can be used to locate a cue in a complex environment.

Acknowledgements

I would like to acknowledge the people that were instrumental in making this work a reality. First, I would like to thank Dr. David Feldheim for his insight and help in making this document a possibility. Second, I would like to thank Dr. Bin Chen for donating multiple animal models and allowing her staff to assist me in my data acquisition, as well as giving me thoughtful advice. I would also like to thank Dr. Laura Schaevitz for her knowledge and expertise concerning animal behavior, her help was integral in answering fundamental questions. Dr. Shinya Ito and Dr. Alan Litke were the driving force behind the silicon probe physiology experiments and I thank them greatly for their contribution to this manuscript. I would also like to acknowledge my lab mates including Jena Yamada, Keily James, Neal Sweeney, and Andreea Nistorica for their expertise, commentary and general insight concerning scientific scholarship. I would also like to acknowledge Dr. Brunhilde Wirth and Dr. John Rubenstein for their donation of the Tra2β conditional knock out animal and the Tbr1 knock out animal respectively. Without the use of these two animal models this

work would not have been possible. I would also like to thank everyone on the Graduate Advisory Committee and in the MCD biology department. Finally, I would like to thank my better half, Serena Sage, for all of her understanding and support.

Chapter 1

Introduction

The human brain contains billions of neurons that form trillions of connections, how these precise connections are formed is a fundamental question in the field of neuroscience (Williams & Herrup, 1988). Wiring defects within the human brain have been implicated in several cognitive disorders including autism, schizophrenia, and other sensory processing disorders (Tye and Bolton, 2013; Kana et al., 2011; Buchman et al. 2014; Chang et al., 2014). The use of animal models has contributed greatly to our basic understanding of developmental neuroscience. The mouse visual system in particular has proven to be of great use in better understanding how specific classes of neurons find their appropriate targets. My thesis work has been devoted to better understanding how output neurons of the retina locate their appropriate targets and the necessity of cortical input in circuit formation, physiology, and behavior.

The mouse visual system is a complex network comprised of the retina, which transforms photons into a chemical signal, and the brain targets of the retina, which convert chemical signals into appropriate behaviors. The retina accomplishes this by sending information to multiple subcortical targets via ~20 distinct types of retinal ganglion cells (RGCs) which are responsible for detecting and transmitting one or more features of the visual scene via distinct parallel circuits. Retinal parallel circuits can be separated into two separate pathways, "image forming" and "non-image forming". The image-forming pathway is comprised of multiple RGC types,

including RGCs that fire action potentials in response to changes in luminance (OFF, ON, ON-OFF) or to movement in a specific direction (ON-OFF direction selective). These two types of RGCs and others send axons to two distinct subcortical nuclei, the dorsal lateral geniculate nucleus (dLGN) located in the visual thalamus and superior colliculus (SC), located in the dorsal region of the midbrain, both known as image forming nuclei. The SC modulates reflexive head and eye movements while the dLGN is the only RGC subcortical target that relays information about the visual scene to the visual cortex (V1), where conscious vision is processed. The non-image forming pathway is comprised of RGCs that express the photopigment melanopsin, creating neurons that are intrinsically photosensitive (ipRGCs) that can fire action potentials independent of connectivity to rods and cones. ipRGCs relay information to multiple subcortical visual nuclei responsible for different behaviors including the olivary pretectal nucleus (OPN) which mediates the pupillary light reflex (Chen et al., 2011), the suprachiasmatic nucleus, intergeniculate leaflet, and ventral lateral geniculate nucleus (SCN, IGL and vLGN), all of which play a role in regulating day-night activity cycles (Harrington, 1997; Hattar et al., 2002; Morin et al., 2003; Cosenza & Moore, 1984) as well as both the nucleus of the optic tract (NOT) and medial tegmental nucleus (MTN) both involved in image stabilization, all of these nuclei regulate non-image forming behaviors (Osterhout et al., 2015).

The proper development of the visual system seems to rely on a multitude of molecular signals to ensure that RGCs target specific subcortical nuclei in a stereotypic manner. How each RGC type picks their appropriate target is not well

understood, but a favorite hypothesis is that target cells express molecules that are selectively recognized by specific RGC types, which promote axon branching and synapse formation. Recent evidence suggest that a variety of cell adhesion molecules are necessary for the proper targeting of various non-image forming nuclei; however, molecules necessary for stereotypic targeting of image forming nuclei have yet to be discovered. (Osterhout et al., 2011; Osterhout et al., 2015; Sun et al., 2015).

In addition to receiving input from the retina, most retinorecipient areas, also receive direct inputs from the visual cortex (V1) that feed back to modulate the gain of the feed-forward projections from the retina (Theyel et al., 2010; Sillito et al., 2006). Output neurons from cortical layer 5 in V1 project to the SC, OPN, and vLGN, while output neurons from cortical layer 6 in V1 innervate the dLGN, again, the only nucleus that projects directly to the cortex (Schmidt et al., 1993; Erisir et al., 1997; Seabrook et al., 2013). The necessity of cortical inputs for proper RGC axon targeting to visual nuclei and visual behaviors is not well understood.

Structure of the retina

The mouse retina is a laminated structure consisting of five distinct neuronal subtypes including: photoreceptors, bipolar cells, horizontal cells, amacrine cells, and retinal ganglion cells (Figure 1). Rods and cones release neurotransmitters causing an action potential to be generated in the inner nuclear layer neurons which is then transmitted via dendrites of the outer plexiform layer to image forming RGCs that propagate action potentials to the appropriate image forming targets (for review see

Hildebrand and Fielder, 2010). ipRGCs are intrinsically photosensitive and can generate an action potential independent of rod and cone connectivity and propagate this signal to the appropriate non-image forming nuclei (Hattar et al., 2002). Recent molecular biology tools have allowed for the almost complete identification of image forming RGCs using a monoclonal antibody that targets Brn3A, a homeobox/POU domain transcription factor and non-image forming RGCs using a monoclonal antibody for the t-box transcription factor Tbr2 (Quina et al., 2005; Sweeney et al., 2014).

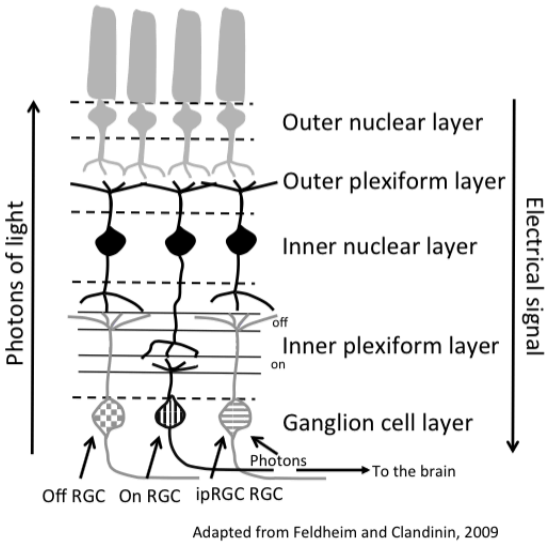

Figure 1. **Simplified schematic of the retina:** the retina is comprised of multiple layers including: the outer nuclear layer consisting of photoreceptors (gray) that capture photons of light and propagate an electrical signal to rod bipolar cell dendrites located in the outer plexiform layer. Rod bipolar cells (black), located in the inner nuclear layer extend dendrites into either the "off" or "on" lamina of the inner plexiform layer (IPL). Retinal ganglion cells (RGCs), located in the ganglion cell layer extend dendrites to either the "on" layer of the IPL (black vertical lines) or the "off" layer of the IPL (grey checkerboard and horizontal lines). On RGCs transmit information concerning the increment of light while off RGCs transmit information concerning the decrement of light. This is a simplified description of the image-forming pathway, ~20 different types of RGCs that are sensitive to various features of the visual scene exist that ultimately compose this pathway. ipRGCs, located in the

ganglion cell layer are intrinsically photosensitive (gray horizontal lines), they do not rely on connections from photoreceptors for excitation and can transmit information about ambient light, these ipRGCs comprise the non-image forming pathway. All of the axons from RGCs form the optic nerve and target various nuclei within subcortical targets.

Retinal ganglion cells and parallel circuits

It is critical to point out that RGCs are comprised of ~ 20 different subtypes in the mouse that all send projections to the brain (for review see Sanes and Masland, 2015). The various types of RGCs are sensitive to specific features of the visual scene and can be distinguished by four different criteria: cellular and dendritic morphology, gene expression profiles, regular spacing patterns, and common physiological properties. All RGCs send an axon to the center of the retina (optic disc); these axons comprise the optic nerve, axons then continue to their specific subcortical target. This neuronal diversity creates more than 20 distinct parallel circuits which can be grouped into either the image forming pathway that drives conscious vision and reflexive behaviors or a non-image forming pathway that dictates non-image forming behaviors including the pupillary light reflex and sleep wake cycles as well as image stabilization.

Timing of retinothalamic circuit formation

Methods, which allows for RGC axon visualization, have revealed the timing and patterns of innervation within subcortical nuclei of the mouse brain (Godement et al., 1999). The dLGN receives contralateral RGC innervation at embryonic day 16

(E16), approximately four days before birth. Ipsilateral projections reach the dLGN and SC two days later at E18. RGC projections continue to fill the entire area of the dLGN until postnatal day 3 (P3). During the next four days of development contralateral and ipsilateral RGC projections segregate into eye specific domains within the dLGN. By the time of eye opening at P15 the dLGN has non-overlapping ipsilateral and contralateral RGC projections within their respective nuclei.

Disruption of eye specific domains in dLGN

Eye specific segregation in the dLGN has been studied at length. Blocking visual thalamus activity with tetrodotoxin causes distinct morphological differences in RGC axon terminations within the dLGN. First, RGCs have expanded arborizations that fail to refine appropriately and second, they fail to remain in their eye specific domain (Stretavan et al., 1988). Disrupting retinal wave activity early in development by the genetic removal of the β2 subunit of the nicotinic acetylcholine receptor in RGCs has been shown to enlarge RGC target zones and leads to impaired eye-specific segregation of RGC inputs within the dLGN (Rossi et al., 2001; Dhande et al., 2011) (figure 2). A large body of evidence exists demonstrating that Eph receptor tyrosine kinases and their ligands, the ephrins, are necessary for the proper targeting of RGCs to the dLGN. Triple ephrin knockout mutants fail to send RGC axons to the proper eye specific regions within the dLGN but refinement and segregation into eye specific domains is uninterrupted (Pfeiffenberger et al., 2005) (figure 2). These data suggest that RGC axon path finding and refinement within the

dLGN is dependent on molecular cues and activity.

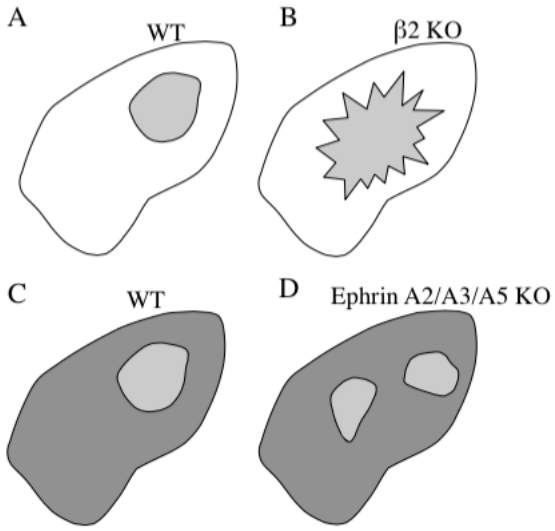

Figure 2 **Defects in eye specific layer location and incomplete refinement of RGC axons in the dLGN:** (**A**) Ipsilateral inputs in the WT dLGN (light gray), (**B**) distribution of ipsilateral inputs into the dLGN of the β2 KO animal (light gray) fail to refine in the absence of retinal wave activity. (**C**) Projections from RGCs in WT animals segregate into eye specific domains, contralateral (dark gray) and ipsilateral (light gray). (**D**) Ephrin A2/A3/A5 mutants have proper eye specific segregation but have defective eye specific locations.

RGC axon targets and associated behaviors

RGC axons target as many as 46 different subcortical structures in the mouse brain, many of which perform complex tasks (Morin & Studholme 2014). Many of the sub cortical targets of RGCs can be separated into two distinct groups: a) non-image forming subcortical targets that are responsible for sleep wake cycles as well as nuclei that drive reflexive behaviors like the pupillary light reflex and image stabilization and b) image forming circuits necessary for processing the visual scene as well as structures necessary for reflexive head and eye movements (figure 3).

The first target of RGCs in the optic pathway is a small hypothalamic nucleus, the SCN (figure 3). This subcortical nucleus is responsible for regulating sleep wake cycles via direct input from ipRGCs. Other targets of ipRGCs along the optic tract are the vLGN and IGL, both of which send a subset of projections to the SCN, which can regulate circadian rhythms in a light independent manner (Amir & Stewart 1996). Loss of ipRGC input within any of theses three nuclei causes defects in sleep wake cycles (Delogu et al. 2012).

The amount of light available at any given time can vary; therefore, the ability to adjust the amount of light that can enter the eye is of significant importance. The nucleus responsible for regulating the constriction or dilation of the pupil, the pupillary light reflex (PLR), is the olivary pretectal nucleus (OPN) (figure 3). The OPN receives direct input from ipRGCs (Panda et al. 2003); loss of ipRGC innervation by either targeted toxin based killing or genetic ablation eliminates the PLR (Guler et al. 2008; Sweeney et al., 2014).

During conscious vision head and eye movements cause images to slide such that without correction the images perceived would be blurry. The accessory optic system (AOS) comprised of a specialized group of RGCs and two distinct subcortical nuclei including the nucleus of the optic tract (NOT) and the medial tegmental nucleus (MTN) adjust horizontal and vertical eye movements that resolve the image slip on the retina and maintain a clear image (Distler & Hoffmann 2011) (figure 3). How different RGC types are involved in this reflex is slowly coming into focus (Kay

et al., 2011).

The dLGN receives direct input from multiple RGC types and is the only subcortical visual structure to send projections to the V1 (Erisir et al., 1997) (figure 3). Genetic tools have made it possible to label distinct subtypes of RGCs and elucidate the organization of visual channels. The Inputs from each of the channels can be organized into the shell and or the core of the dLGN, and with each receiving different types of RGC input. For instance, the shell receives all four types of direction selective RGC input (all four cardinal directions) (Kim et al. 2008, 2010; Huberman et al. 2009; Kay et al. 2011; Rivlin-Etzion et al. 2011), while the core receives input from alpha RGCs, which respond to center surround stimuli but not direction as well as ipRGCs (Huberman et al. 2008; Brown et al. 2010; Ecker et al. 2010) (figure 4). This data suggests that while the dLGN is not a laminated structure like in primates there is a distinct separation and organization of RGC inputs into the shell and core regions. The dLGN is the only subcortical structure to send projections to V1 and recent studies have uncovered four different types of relay cells that reside within the dLGN. These relay cells are akin to those found in primates and include the X, Y and W type as well as local inhibitory neurons (Krahe et al. 2011). These relay cells also preferentially reside in different regions of the dLGN with W-like cells residing in the shell along with direction selective RGCs and Y-like cells in the core with RGCs that respond to center surround stimuli and ipRGCs (figure 4) while X-like cells and interneurons are found throughout the entire dLGN (Piscopo et al. 2013). Anywhere from one to six RGC axons converge onto a single thalamic relay

cell and influence the dLGN cell responses, but whether this interaction sharpens visual features remains unknown (Jaubert-Miazza et al. 2005). It is possible that RGCs that target the core do so because they synapse with Y-like cells or a molecular matching code could exist that dictates the appropriate targeting but the answer to this question remains unknown.

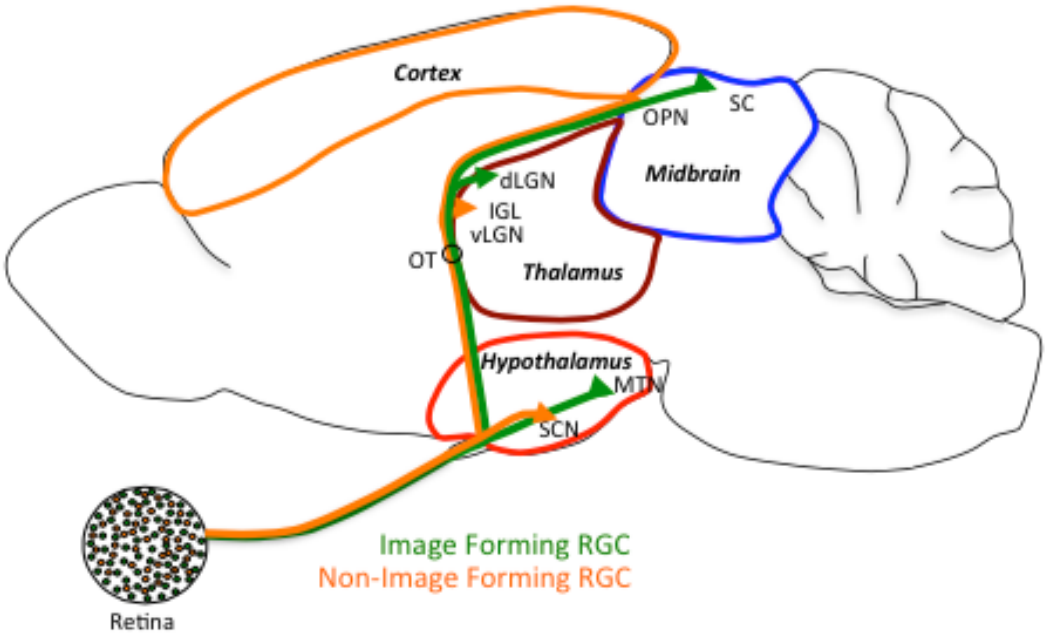

Figure 3. **Sagittal view of the mouse visual system**: The retina contains multiple subtypes of RGCs that can be grouped into two distinct populations of RGCs that comprise two different parallel pathways. Image-forming RGCs (green) target the MTN, dLGN, and SC while non-image forming RGCs (orange) target the SCN, vLGN, IGL, and the OPN.

The SC or optic tectum in lower vertebrates, a midbrain structure, receives and integrates sensory information directly from RGCs, V1, and somatosensory cortex (S1). All three modalities of sensory information are integrated and the

appropriate reflex head and eye movement is elicited via connections with the brain stem (May 2006). Recent advances in genetic labeling tools have made it possible to visualize distinct subsets of RGCs that target the SC. It has been demonstrated that RGCs that respond to object motion as well as ON-OFF and OFF direction selective RGCs target the upper portion of the SC and lateral shell of the dLGN while alpha RGCs, which respond to a brief offset of light, and ipRGCs project to a deeper layer of the SC and the medial core of the dLGN (Huberman et al., 2008; Huberman et al., 2009; Kay et al., 2011; Ecker et al., 2011) (figure 3). This unique input suggests there are multiple channels within the SC that separate into distinct layers although the molecules responsible for dictating RGC laminar choice within the dLGN and SC remain unknown.

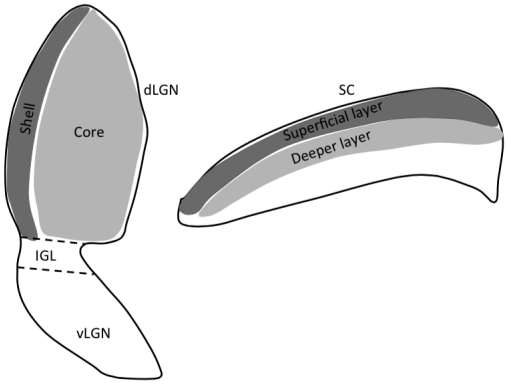

Figure 4. **dLGN and SC can be separated into distinct layers that receive input from different types of RGCs:** The shell of the dLGN contains W-like relay cells and receives input from ON-OFF direction selective RGCs that also terminate within the superficial layer of the SC (dark gray). The core of the dLGN contains Y-like cells and receives input from ipRGC and alpha RGC that also terminate in deeper layers of the SC. (Adapted from Huberman et al., 2008)

Molecules necessary for RGC axon targeting in the visual system

The establishment of functional neural circuits involves neurons sending axonal projections long distances to specific targets. Axons accomplish this by expressing specific proteins on the surface of their growth cone. These proteins are membrane bound and interact with other membrane bound molecules or molecules secreted into the local environment, and these signals can act as either an attractant or repellant. Five families of these molecules have been identified and they include Semaphorins, Netrins, Slits, Repulsive guidance cues, and Ephrins (for review see Battum et al., 2015). Several cognitive disorders including autism, schizophrenia, and other sensory processing disorders are believed to be the result of improper neuronal axon targeting (Tye and Bolton, 2013; Kana et al., 2011; Buchman et al. 2014; Chang et al., 2014).

Investigations in the mouse visual system have revealed numerous molecules necessary for proper axon guidance. Recent work uncovered evidence that in the absence of Reelin, an extracellular matrix glycoprotein, ipRGCs fail to target the IGL (Su et al., 2011). Loss of function and gain of function experiments have demonstrated that contactin 4, a (GPI)-anchored neuronal membrane protein, as well as one of its binding partners, amyloid precursor protein (APP), are required for RGCs to properly target the nucleus of the optic tract (NOT) a key component of the accessory optic system (AOS), necessary for image stabilization (Osterhout et al., 2015). Cadherins have been shown to be necessary for RGC targeting to the optic

tectum in lower vertebrates (Inoue and Sanes, 1997). New evidence suggests that the calcium dependent adhesion molecule, Cadherin-6 (Cdh6) is necessary for ipRGCs to target the non-image forming nuclei. In Cdh6 knockout animals, ipRGCs fail to properly terminate within the OPN. Another example of the necessity of a specific axon guidance molecule is recent data that suggest the transmembrane protein semaphorin 6A (Sema6A), which is expressed in a subset of ON DS RGCs (ON-DSGCs) is required for RGC axon targeting to the medial terminal nucleus (MTN) of the AOS (Sun et al., 2015). These data demonstrate that specific adhesion molecules are necessary for distinct subsets of RGCs to find their proper targets. Currently, all of our knowledge of axon targeting defects within the mouse visual system comes from phenotypes within non-image forming nuclei, the field is still eagerly awaiting the first axon guidance defect in either the dLGN or the SC.

Mouse visual system receives cortical input.

In addition to getting input from the retina, most retinal recipient areas also receive direct input from the visual cortex. Cortical neurons send feedback information that modulates the excitability of the feed-forward projections from the retina (Theyel et al., 2010; Sillito et al., 2006). In the mouse, RGC axons comprise ~10% of the total connections in the dLGN while descending feedback projections from cortical layer 6 make up ~30% of the input (Krahe et al. 2011). Relay cells in the dLGN send ascending projections to cortical layer 4 of the visual cortex comprising 8-10% of the input, while the descending projections from layer six send

collaterals to layer four of the visual cortex, these interactions comprise a feedback loop thought to modulate visual perception and comprise 45% of the input (Erisir et al., 1997; Sillito et al. 2006) (Figure 5). Descending cortical inputs that target non-image forming nuclei including the OPN, IGL, and vLGN arise from layer 5 of the visual cortex (Schmidt et al., 1993) (Figure 5).

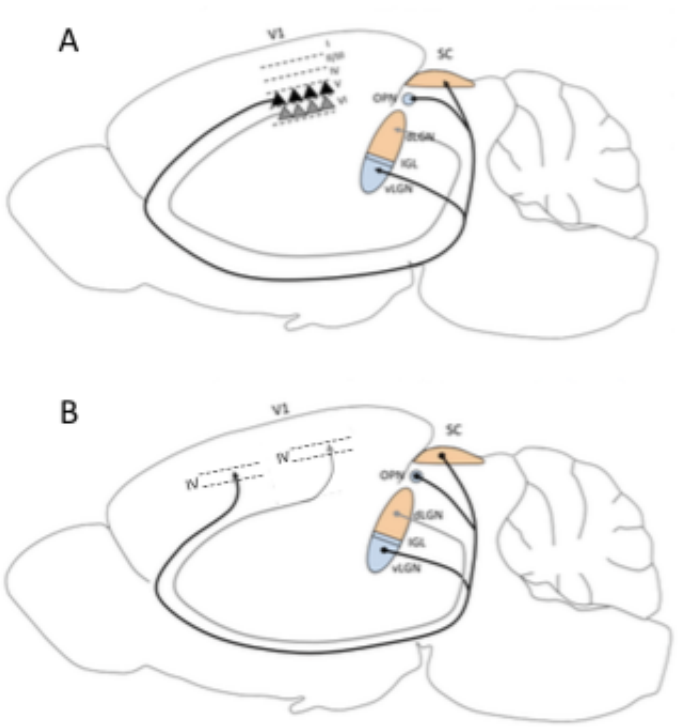

Figure 5. **Cortical circuitry of mouse visual system:** Sagittal view of adult mouse brain. (**A**) Descending cortical layer 5 projections target the vLGN, IGL, OPN and SC (black) and descending cortical layer 6 projections target the dLGN (gray). (**B**) Ascending cortical projections from IGL, vLGN, OPN, and SC target layer 4 in non-visual cortex targets (black) and ascending cortical projections from the dLGN target layer 4 of V1 (gray).

Recent work using the Golli-τ-EGFP mouse, a transgenic line that fluorescently labels layer 6 cortical neurons selectively, has demonstrated the timing and innervation patterns of cortical layer 6 projection neurons within the mouse visual

thalamus (Seabrook et al., 2013). RGCs innervate the visual thalamus between E16 and E18 and are already present when cortical layer 6 neurons transcend the internal capsule (IC) and innervate the ventrobasal nucleus by post-natal day 2 (P2) and stall at the medial border of the dLGN (Figure 6). Cortical layer 6 axons begin to enter the dLGN by P6 but do not target the vLGN, except for a small amount of innervation in the center (Seabrook et al., 2013). In mice that have been enucleated (eyes removed) at late perinatal stages thus eliminating all RGC axons or in transgenic mice that fail to develop RGCs cortical layer 6 axons fail to wait at the medial border of the dLGN (Seabrook et al., 2013; Wang et al., 2001). The disrupted timing of cortical innervation in both of these models suggests that RGC axons are exerting control over when cortical layer 6 axons can innervate the dLGN. Indeed, new evidence suggests that aggrecan, a repulsive chondroitin sulfate proteoglycan, can inhibit cortical layer 6 axonal outgrowth in vitro and this molecule prevents axons from prematurely entering the dLGN (Brooks et al., 2013). It is also hypothesized that RGCs inhibit relay cells in the dLGN from expressing the aggrecan degrading enzyme aggrecanase, demonstrating that RGC innervation plays a critical role in the timing of cortical layer 6 axon innervation within the dLGN (Brooks et al., 2013) These data taken together demonstrate critical timing patterns of RGC innervation within the visual thalamus, which exert control over cortical layer 6 innervation. What is not well known is whether lack of cortical input plays a role in RGC timing and patterns of innervation within the dLGN.

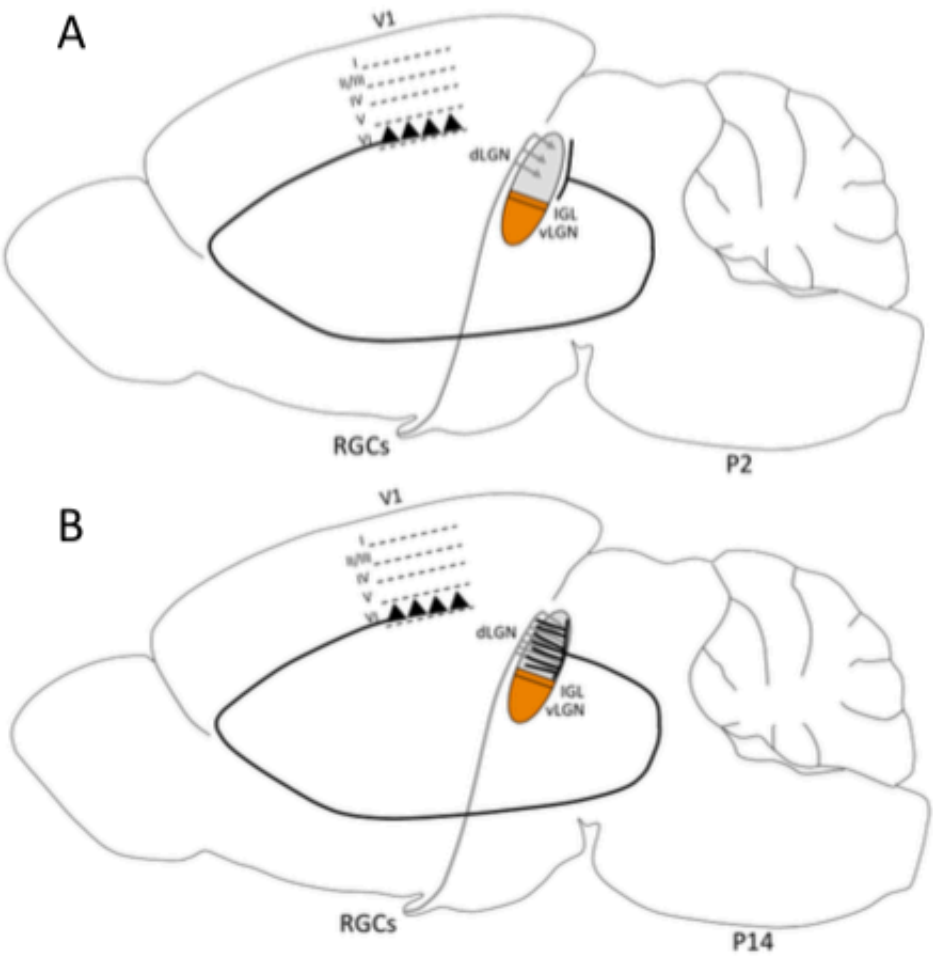

Figure 6. **Timing of layer 6 cortical innervation within the dLGN:** (**A**) RGC projections occupy the dLGN by postnatal day 2 (P2), cortical layer 6 neurons have arrived at the medial border of the dLGN but fail to innervate. (**B**) RGC axons and cortical layer 6 projections completely innervate the dLGN by P14, a few days before the animal opens its eyes. (Adapted from Seabrook et al., 2013)

Summary

The mouse visual system has become an increasingly useful tool to study the formation of neural networks as well as the molecules necessary for this precise formation. Excellent behavioral tests also exist to better understand the cosequences of improper axonal targeting. Recent data has demonstrated the timing and location of RGC innervation within subcortical targets as well as innervation patterns of multiple output layer neurons from the visual cortex (fig. 7).

Despite a wealth of knowledge about mouse visual circuitry and the associated behaviors, little is know about the necessity of cortical input not only during the development of the mouse visual system but also its necessity for image forming and non-image forming behaviors. By utilizing a mouse that lacks a neo-cortex, thus cortical input within visual nuclei, my goal was to characterize RGC inputs within the developing mouse visual system and to investigate how this loss affects normal innervation patterns of RGCs within visual nuclei. Also, because of recent evidence demonstrating the need for RGC input within the visual thalamus to regulate the timed innervation of cortical inputs, I was excited to investigate the converse, the need for cortical input during RGC targeting of the visual thalamus. My work further allowed me to test whether cortical circuitry is necessary for perception and if so, does that perception allow for the ability to navigate a complex environment.

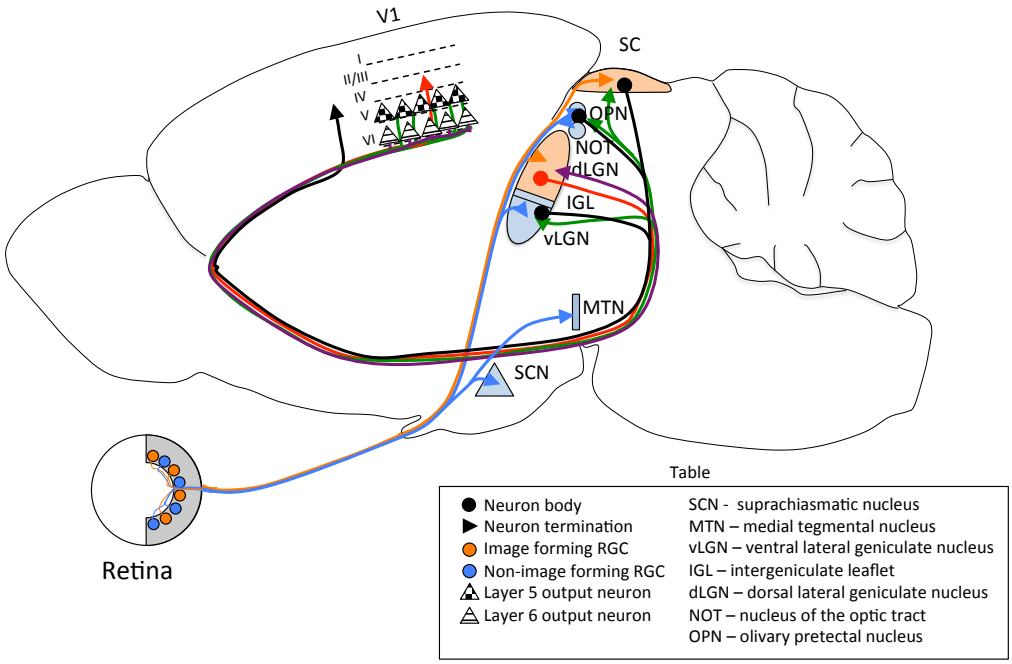

Figure 7. **Schematic of the mouse visual system including descending and ascending cortical projections:** Non-image forming RGCs (blue) target distinct subcortical nuclei including: SCN, MTN, vLGN, IGL, NOT, and OPN. Image forming RGCs (orange) target distinct subcortical nuclei including: the dLGN and SC. Descending cortical layer 5 neurons from V1 (checker board cell bodies, green axons) target the vLG, IGL, OPN, and SC while descending layer 6 cortical neurons from V1 (horizontal line cell bodies, purple axons) only target the dLGN. The dLGN sends ascending relay neuron projections directly to layer 4 of the visual cortex (red) while ascending projections from vLGN, OPN, and SC send projections to layer 4 (black) in non V1 cortical nuclei.

Chapter 2

Methods

Transgenic mice

Tra2β floxed animals were obtained from Dr. Brunhilde Wirth (University of Cologne) and Dr. Bin Chen (UC Santa Cruz, Roberts et al., 2013). The Emx1-Cre mouse line (stock#005628) and the Td-Tomato reporter line (stock#007905) were obtained from The Jackson Laboratory. The Isl2-GFP mouse line was generated at UCSC as described (Triplett et al. 2014). Tbr1 KO animals (Bulfone et al., 1998) were obtained from Dr. John Rubenstein, UC San Francisco) and Dr. Bin Chen. Mice were genotyped by PCR of tail DNA using the following oligonucleotides: GFP (5'-CCTACG GCGTGCAGTGCTTCAGC-3' and 5'CGGCGAGCTGCACGCTG CGT CCTC- 3′); Tra2β (5'AAGGCGTTCTAGATC AAAGTCCAG-3' and 5'-GTCGA CGAGAGGGCACGAGAG GACAATC-3'); Emx1-Cre WT for (5'-GTGC CATC ATGAAGGATGC-3') Emx1-Cre for (5'-GT ATTTGGTTTAGAGTTT GGC-3') and rev (5'-GGGGGACATGAGAGGATGT CAC-3'); Tbr1 KO (5'-GTGGCTAG AGCACGA-CGGAGAGC-3' and 5'-CTT CTTGACGAGTTCTTCTGA-3'), Tbr1 WT (5'-GGTCGGAGAACCAGTCAGTG -3' and 5'-GGGAGAAGGGAAGAC GTA GG-3'); WT (5'-AAGGGAGCTGCAGTGG AGTA-3' and 5'-CCGAAA ATCTGTGGGAAGTC-3') and TdTomato (5'-GGC ATTAAAGCAGCGTATCC-3') and 5'-CTGTTC CTGTACGGCATGG-3'). All procedures were performed in accordance with the UCSC Institutional Animal Care and Use Committee.

Tracing RGC axons

To anterograde label RGC axons, P0 mice were anaesthetized on ice for 5 minutes; adult animals were anaesthetized using a constant flow of 1% isoflurane. Approximately 1μL of fluorescently conjugated cholera toxin subunit B (CTb-488 or CTb-555, Life Technologies, Carlsbad, CA, USA) (2 mg/mL in PBS) was injected into the vitreous of the eye using a pulled glass pipette, previously beveled with a micro-grinder (Microdata Instruments Inc. MFG-5) using a Picospritzer III (Parker Instruments, Carlsbad, CA, USA) set at low pressure and 5ms pulse duration. After two days animals were sacrificed and intracardially perfused with phosphate buffered saline (PBS) containing 4% paraformaldehyde (PFA). Brains were dissected out and placed in 4% PFA overnight at 4^{O}C, then cryoprotected by equilibrating in 30% sucrose in PBS overnight at 4^{O}C. 100μm coronal brain sections were acquired using a HM430 frozen microtome (Thermo Fisher). Imaging was performed with an Olympus BX51 epifluorescent microscope equipped with QImaging Retiga EXi digital camera or a Leica Wide-field DM5500. The distances of nuclei were calculated using ImageJ.

Immunohistochemistry

Adult male and female mice were sacrificed and perfused intracardially with PBS and 4% PFA. Eyes were removed from the skull and placed in 4% PFA for 10 min at room temperature (RT). For whole mount preparations, retinas were dissected

out of the eyes and placed in 4% PFA for 1 h. For cryosectioning, the lens and vitreous were removed and the whole eye was equilibrated in 30% sucrose overnight at 4°C. Whole eyes were then inserted into Tissue-Tek OCT Compound (Sakura Finetek), frozen using dry ice. 20 mm sections were obtained from a CM1520 Cryostat (LeicaMicrosystems) at -22°C and collected on glass plus slides. Sections were allowed to dry for 12 h at room temperature. For immunohistochemistry, the sections were rehydrated in PBS for 5 minutes. Retinas and retinal sections were then placed in blocking solution (5% goat serum, 0.25% Triton X-100 in PBS) for 1h at RT. The following antibodies were diluted 1:1000 in blocking solution and retinas were placed in solution at 4^{O}C overnight: Tbr2 chicken polyclonal (Lifespan), Brn3a goat polyclonal (Santa Cruz Biotechnology) or ChAT rabbit polyclonal (Millipore). Retinas were washed in phosphate buffered saline with 1% Triton X-100 (PBST) for 10 min three times. The retinas were then incubated with the applicable secondary antibody 1h at RT. Retinas were washed with PBST for 10 minutes 3 times and a glass coverslip was mounted with Fluoromount (Southern Biotech). Imaging was performed with an Olympus BX51 epifluorescent microscope equipped with QImaging Retiga EXi digital camera.

Histochemistry

Adult (P40 to P60) mice of each sex were sacrificed and perfused intracardially with PBS and 4% PFA. Brains were removed and placed in 4% PFA overnight at 4ºC then soaked in a 30% sucrose solution overnight at 4ºC. Whole

brains were then inserted into Tissue-Tek OCT Compound (Sakura Finetek), placed on dry ice for 30 min, and 20μm sections were obtained from a CM1520 Cryostat (LeicaMicrosystems) at -22°C and collected on glass plus slides (Superfrost plus, Thermo Scientific). Sections were allowed to dry for 12 h at room temperature. For 4',6-diamidino-2-phenylindole (DAPI) staining, the sections were rehydrated in PBS for 5 minutes and placed in a 1mg/ml solution of DAPI in PBS for 5 minutes before coverslipping. Those stained for NISSL were dehydrated, incubated in 100% xylene and rehydrated by descending ETOH then stained with 2% cresyl violet as described (Kadar et al., 2009). For cytochrome oxidase staining adult brains were flattened between glass slides in 4% PFA overnight then placed in 30% sucrose overnight at 4ºC. 100μm coronal brain sections were acquired using a HM430 frozen microtome (Thermo Fisher). Sections were placed in a solution of 5% sucrose, 0.03% cytochrome C, 0.02% catalase, 0.05% DAB in phosphate buffer (0.5M NaH_2PO_4, 0.15 M Na_2HPO_4, pH 7.4) overnight at 37ºC, quenched with 0.1% NaN_3, and coverslipped (Triplett et al., 2012). All imaging was performed with an Olympus BX51 epifluorescent microscope equipped with QImaging Retiga EXi digital camera or Keyence BZ-9000.

In situ RNA hybridization

In situ probes for ephrin-A5 (nucleotides 102–682 of the open reading frame) and EphA7 (nucleotides 721–1193) were used to make antisense and sense digoxigenin labeled RNA probes. P2 whole brain 20μm coronal sections were

acquired using a CM1520 Cryostat (LeicaMicrosystems) and *in situ* hybridization was done as previously described (Feldheim et al. 1998). Stained sections were photographed using a Keyence BZ-9000.

Silicon probe in-vivo electrophysiology

Silicon probes were provided by the Masmanidis lab at UCLA (Du et al. 2011). We used two-shank 64 or 128 channel probes. Electrodes were arranged in 3 columns on each shank with 50 μm vertical spacing within each column.

Our procedure is based on (Niell and Stryker, 2010). Experiments were performed on adult (age 2-6 month) male mice. Animals were maintained on a 12 hr light/ 12 hr dark cycle. Experiments were performed during the light phase of the cycle. 3 WT and 3 Tra2β cKO mice were used for the recordings. The mice were trained for at least 30 minutes each day for 4 days prior to being used for recording.

The silicon probe recording was performed while the mouse was awake-behaving on a spherical treadmill. On the day of recording, the mouse was anesthetized with isoflurane (3% induction, 1.5-2% maintenance), and a craniotomy (~1.5 mm diameter) was performed at a site that was 0.6 mm lateral from the midline (left hemisphere) and 3.7 mm posterior from the bregma. The probe was inserted through the cortex to the SC; the first electrode in the SC was located 1000-1500 μm from the cortical surface. The probe was then moved forward by ~300 μm to cover a larger area of the SC. Activity in the SC was identified by displaying either an ON or OFF flashing spot on a computer monitor and detecting neuronal responses in a certain

location of the visual field. The visual stimulus monitor was placed 25cm away from the right side of the mouse, thus covering the receptive fields of neurons on both of the shanks. After the probe was inserted to a final position, it was allowed to settle for at least 30 minutes; only then were visual stimuli shown to obtain stable single-unit recordings. During the recording, the mouse was allowed to behave freely on the treadmill.

Three different visual stimuli were used to evaluate visual responses of the SC neurons: 1) *10˚ diameter flashing circular spots on a 10 x 7 grid with 10˚ spacing:* the 500 ms flashes were either ON (white) or OFF (black) on a gray background and a 500 ms gray screen was inserted after each stimulus presentation. Stimulus contrast and location on the grid were chosen in a random order, and each pattern was repeated 12 times. This stimulus is similar to what was used in (Wang et al., 2010) with a few differences in parameters. 2) *Black and white white noise stimulus:* a random white noise movie with a 60Hz refresh rate was presented for 30 minutes. The size of the stimulus panel was 6˚, and each panel was randomly assigned either black or white at a given time. 3) *Drifting sinusoidal gratings*: the parameters were the same as those used in (Niell and Stryker, 2008). Briefly, we used sinusoidal gratings moving in 12 directions with 0.01-0.32 cycles/˚ (cpd) spatial frequencies with a logarithmic scale with a factor of 2 as an interval. Temporal frequency and duration were 2 Hz and 1.5 s, respectively. In addition to these stimuli, an alternating checkerboard stimulus (4 cpd square wave, alternating at 0.5 Hz) was used to determine the current sink in superficial SC (Zhao et al., 2014). All visual stimuli

were synchronized with digital pulses sent from the stimulus computer to the data acquisition system.

For spike-sorting and local field potential analysis, we used custom-designed software as described (Litke et al., 2004). Briefly, a level 5 discrete wavelet filter (cutoff frequency ~313 Hz) (Wiltschko et al., 2008) was applied to the recorded data. The high-pass part was used for spike-sorting to find single units and filtered data was also subjected to motion artifact removal; the low-pass part was used for a current source density analysis. The average motion artifact shape was estimated by averaging signals from all the recording channels. The estimated artifact was then subtracted from each channel with a multiplication factor that reduces the noise level of the channel most effectively (determined by the least-squares method). In the following steps, in addition to what was described in (Litke et al., 2004), we used Bayesian Information Criterion to optimize the numbers of clusters in the expectation maximization step (Fraley, 1998) and also introduced Isolation Distance (>20) and L-ratio (<0.1) as criteria of a good cluster (Schmitzer-Torbert et al., 2005).

Current source density (CSD) for each shank was calculated as described in (Niell and Stryker, 2008) using the middle column of electrodes, while the center of gravity (CoG) of the current sink (negative part of CSD) was used to estimate the center of visual response in the superior colliculus (see also supplemental information of (Zhao et al., 2014). In order to restrict analysis to superficial SC neurons, we only used neurons that have a depth ±250 μm from the CoG of the current sink.

Significance of the response was evaluated at each grid location of the flashing spot stimulus. First, the post-stimulus time histogram was calculated using a 50 ms bin size. If the firing rate of a bin exceeds the threshold value, $\boldsymbol{\overline{F} + 5 * \sigma}$, where $\boldsymbol{\overline{F}}$ is a mean firing rate of the neuron during entire flashing spot stimulus, and σ is a standard deviation of the firing rate based on Poisson statistics, the response is considered significant. If a cell had significant responses to the white or black flashing spot only, the cell was considered to be an ON or OFF cell, respectively; if it had significant responses to both white and black spots, it was considered to be an ON-OFF cell. Receptive field diameters were estimated by the number of significant grid locations; each location accounted for an area of 100 square degrees. The diameter was approximated using a circle that has the same area as the actual receptive field area. Namely, $\boldsymbol{d = 2\sqrt{A/\pi}}$, where d and A are the diameter and the area of the receptive field, respectively.

The white noise receptive fields were measured for each neuron by calculating spike-triggered averages (STAs) to the visual stimulus as described in (Chichilnisky, 2001). The response was considered significant if an STA had a non-flat time course (tested by reduced $X^2 > 4$). If the first peak of the STA is positive the cell is considered an ON cell, if the STA is negative it is considered an OFF cell.

Direction and orientation selectivity were analyzed with the same methods found in (Niell and Stryker, 2008). Briefly, Direction Selective Index (DSI) is a difference over sum (DoS) of responses to the preferred direction and its opposite direction; Orientation Selective Index (OSI) is a DoS of responses to the preferred orientation

and its orthogonal orientation. DSI ≥ 0.5 was used as a criterion of direction selective cells; OSI ≥ 0.5 & DSI < 0.5 were used as criteria of orientation selective cells.

Fear Conditioning

The ability to sense light stimuli was assessed using an automated fear conditioning system for mice (Coulbourn Instruments, Allentown, PA, USA) with the following parameters: Day 1, acquisition: 3 minute habituation in chamber A, followed by 10 light shock pairings with an average inter trial interval of 120 seconds consisting of 8 seconds of flashing light, 0.5 second on 0.5 second off, followed by 2 seconds of flashing light paired with 0.3mA foot shock. Day 2, retention: 3 min habituation in chamber B, followed by 3 minutes of continual flashing light. Freezing during cued retention was recorded by an automated system (Graphic State3.0 software; Coulbourn Instruments). Prior to statistical analysis, all freezing intervals greater than 2 seconds in length during acquisition of cued retention were summed in 60-second intervals.

Cued Swim Maze

The water maze consisted of a round white tank 4 feet in diameter and 2 feet tall filled with ~10 inches of water. All external visual cues were removed. The water temperature was maintained at ~22°C during all trials. Animals were tracked using AnyMaze (Stoelting) video tracking system. On day 1, four trials were conducted, the mouse was placed in the pool at one of four defined compass points around the edge

of the pool and a clear platform was placed in one of four defined quadrants. Mouse placement in the pool and platform location varied across each trial. The mouse was given 60 seconds to find the platform, which was marked with a blue visual cue. Upon reaching the platform, the mouse was left on the platform for 5 s before being returned to its home cage. If the mouse was unable to find the platform it was placed on the platform for 5 seconds. On day 2, the preceding procedure was replicated, but this time the cue was a flashing white light. On day 3, the preceding procedure was replicated for the first two trials. During the last two trials, the cue was removed. Latency to the platform was used to assess the mouse's perceptive ability. Tra2β cKO animals can display a severe circling phenotype that can limit their ability to orient during the water maze task. Some Tra2β cKO animals displayed a severe circling phenotype that wasn't conducive to searching for a cue. The average number of rotations per WT animal across all three trials was 23.8 ± 11.7 S.D., any animal that rotated more than 150 times across all three trials was removed from the data analysis (n=3).

Pupillary light response

To measure the pupillary light response, both male and female mice were dark adapted for 1 minute under infrared light. While under infrared light, mice were filmed using a Sony Handycam DCR-HC96 for 10 seconds to obtain a baseline reading. This was followed by exposure of the contralateral eye to 460 nm LED light for 30 seconds at the high-light condition (2.9 mW/cm2). Then, following several

minutes in dark conditions, the animals were exposed to low-light condition (172 mW/cm2). Light levels were controlled using neutral density filters. Movies were converted into still photos using MPEG Streamclip and the percent of pupil constriction was calculated using ImageJ. The percent pupil constriction was calculated as the difference in pupil size between dark-adapted and light-exposed eyes.

Locomotor activity

Activity was measured in 12h dark/light cycles for 60h. The activity chamber consisted of a clear acrylic cage (43 X 22 cm) containing a 3x8 array of photo beams mounted 2.5 cm from the chamber floor. The photobeam breaks were recorded using PAS software (San Diego Instruments). Each mouse was placed individually into a cage and the number of photo beam breaks was monitored for 60h starting at 18:00 h. The total number of photo beam breaks per 1-h interval was recorded.

Chapter 3: Investigating the necessity of cortical inputs during development of the mouse visual system

Introduction

The brain detects and processes sensory information using parallel circuits, each of which processes specific aspects of the environment that is then integrated to encode perception and issue appropriate behaviors (Wassle, 2004). Understanding how these circuits form during development is important because a number of developmental disorders are thought to arise from the mis-wiring of brain circuitry; (Tye and Bolton, 2013; Kana et al., 2011) furthermore, once elucidated, these same mechanisms used to form connections can be utilized to re-wire connections after injury or disease.

The visual system is an attractive model used to study the development of circuit formation. In the mammalian visual system the retina transforms the visual scene into approximately 20 different channels, each represented by a unique type of retinal ganglion cell (RGC) (Masland, 2012). All RGC types send axonal projections to specific subcortical retinal recipient areas that are responsible for executing reflexive and planned behaviors (Dhande and Huberman, 2014). For example, some RGC types fire action potentials in response to changes in luminance (OFF, ON, ON-OFF) or to movement in a specific direction (ON-OFF direction selective). These types send axons to the dorsal lateral geniculate nucleus (dLGN) and superior colliculus (SC), referred to as image-forming areas because of their roles in reflexive and planned movements. Intrinsically photosensitive RGCs (ipRGCs) and some

conventional RGCs have axons that project to nuclei involved in specific non-image forming behaviors. Such regions include the olivary pretectal nucleus (OPN), which regulates the pupillary light reflex (Chen et al., 2011), and the suprachiasmatic nucleus, inner geniculate leaflet, and ventral lateral geniculate nucleus (SCN, IGL and vLGN), all of which play a role in regulating day-night activity cycles (Harrington, 1997; Hattar et al., 2002; Morin et al., 2003; Cosenza & Moore, 1984). How each RGC type targets a specific nucleus in the brain is not well understood, but a favorite hypothesis is that target cells express molecules that are selectively recognized by specific RGC types, thereby promoting axon branching and synapse formation (Osterhout et al., 2011; Osterhout et al., 2015; Sun et al., 2015).

In addition to getting input from RGCs, most retinal recipient areas also receive direct inputs from the visual cortex that feed back to modulate the feed-forward projections from the retina (Theyel et al., 2010; Sillito et al., 2006). Layer 5 neurons in the visual cortex project to the SC, vLGN, and OPN, while layer 6 neurons innervate the dLGN, the only nucleus that projects directly to the cortex (Schmidt et al., 1993; Erisir et al., 1997; Seabrook et al., 2013). Whether these inputs are required for proper RGC axon targeting during development and target cell receptive field properties is not known.

Here we investigate the developmental and functional changes that occur in the mouse visual system when mice develop without a large portion of their cortex. To do this we examined the retinal projections in Tra2β floxed (Tra2β conditional knockout [cKO]); *Emx1*-cre transgenic mice, which lack most of the cortex, including

the entire visual cortex (Gorski et al., 2002; Mende et al., 2010; Roberts et al., 2013). We find that Tra2β cKO mice have an almost complete loss of RGC axon input into the dLGN, but normally innervate many other RGC targets. RGC axons also fail to completely innervate the dLGN in mice that lack cortical layer 6 projections to the dLGN. This suggests that retinal-geniculate target selection requires a cortical axon derived signal that attracts RGC axons to the dLGN.

Layer 5 neurons project to the SC, and we find that while the lack of cortical inputs does not prevent RGC innervation in the SC, it leads to changes in the visually derived response properties of collicular neurons. Finally, we show that when mice develop without a cortex they are still able to perform a number of vision-dependent tasks.

Results

Cortical innervation is necessary for targeting image-forming RGC axons to the dLGN.

To determine if cortical development is required for normal RGC axon targeting, we anterograde traced the RGC axonal projections in Tra2β $^{flox/flox}$; Emx1-Cre^{+} mice (hereafter referred to as Tra2β cKO mice). In these mice Tra2β is deleted from most of the developing cortex, and cortical progenitor cells that lack Tra2β apoptose (Roberts et al., 2013). Although viable, this mouse lacks ~85% of the neocortex, and has a complete loss of the visual cortex (Roberts et al., 2013). A comparison of brains from wild type (WT) (Fig. 10 A) and Tra2β cKO (Fig. 8 B) mice demonstrates the severe loss of cortex in the Tra2β cKO (Roberts et al., 2013). To determine whether the lack of a cortex affects RGC axon targeting, RGC axons from WT and Tra2β cKO mice were labeled via an injection of cholera toxin subunit B conjugated to fluorophores (CTb-488 and CTb-555) into each eye two days prior to harvesting the brains. Coronal sectioning of the brain allows the visualization of both contralateral and ipsilateral RGC axons in all of the retinal recipient nuclei (Pfeifenberger et al., 2006; Triplett et al., 2014). While the SCN, OPN, and SC have no significant differences in RGC axon distributions between the two genotypes (Fig. 8 C-H), there are dramatic changes in the innervation pattern of RGC axons in the visual thalamus, including the vLGN, IGL, and dLGN (Fig. 8 I-N). Most dramatically, the dorsal medial portion of the dLGN lacks RGC axons in the Tra2β cKO. This void area of the dLGN can be detected as early as P2, an age before

cortical innervation of the dLGN is thought to begin (Seabrook et al., 2013), and loss of innervation continues into adulthood. The ventromedial to dorsolateral extent of the inputs within the entire LGN are reduced significantly in the Tra2β cKO mutants even at early time points (Table 1, Fig. 8 P). The area of innervation of RGC axons in the vLGN of Tra2β cKO is significantly greater along the medial-lateral axis at each age tested (Table1, Fig. 8 Q). We also find that compared to WT, the thickness of the optic tract (OT) dorsal to the dLGN is significantly enlarged in Tra2β cKO animals starting at P7 (Table1, Fig. 8 R). Taken together, these data show that complete RGC innervation of the dLGN requires a developing cortex.

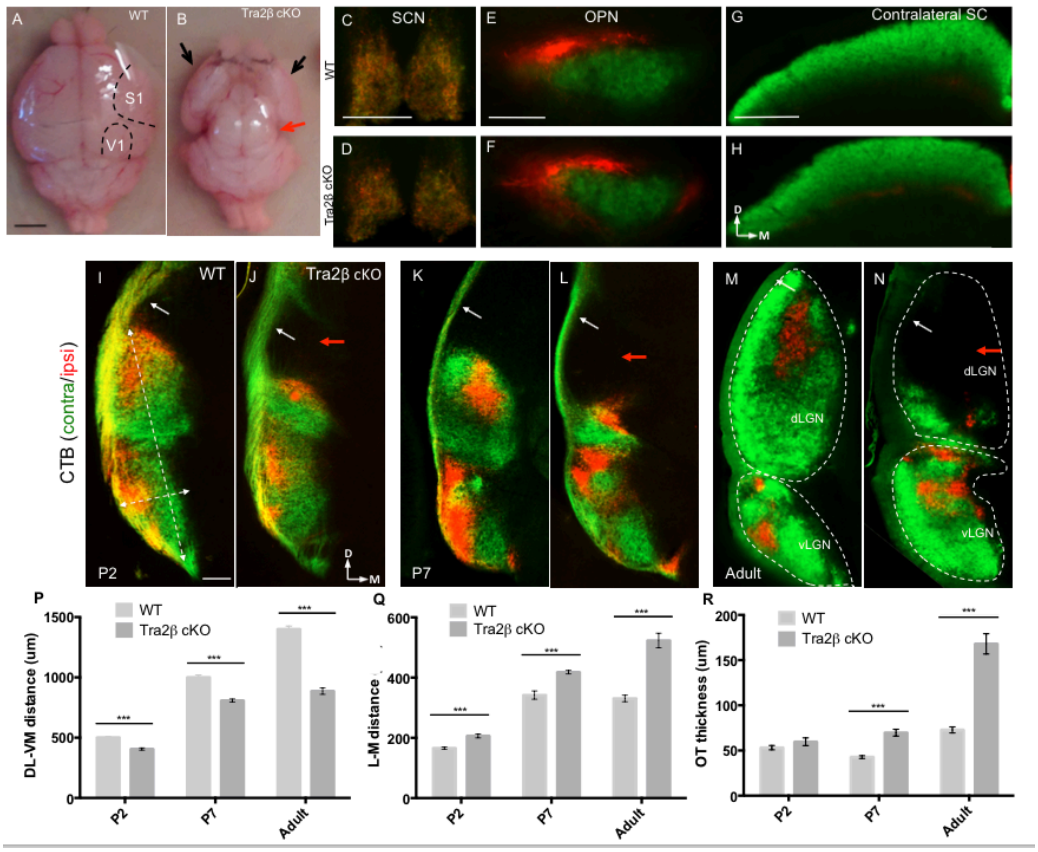

Figure 8. **Emx1-Cre;Tra2β mutant mice have severe cortical tissue loss and loss of RGC inputs to the dLGN.** Dorsal view of Wild type (**A**) and Tra2βflox/flox; Emx1-Cre (Tra2β cKO) mutant (**B**) adult brains. Mutants show complete loss of dorsal and medial cortex. Red arrow points to completely exposed superior and inferior colliculi. Black arrows indicate the lateral portion of cortex that remains in the mutant. (**C-H**): RGC projections to subcortical visual nuclei were labeled by injection of CTb-488 (green), and CTb-555 (red) into each eye of adult WT and Tra2β cKO animals. RGC axons in both wild type and Tra2β cKO project to non-thalamic retinorecipient nuclei: SCN (**C**,**D**), OPN and (**E**,**F**), and SC (**G**,**H**). (**I-N**) Left hemisphere of retinogeniculate projections in WT and Tra2β cKO at three different ages: P2 (**I**,**J**), P7 (**K,L**), and adult (**M,N**). Tra2β cKO dLGN lacks contralateral (green) and ipsilateral (red) innervation (red arrows) that is evident by P2. White dashed line indicates total area of both vLGN and dLGN in adult animals. Tra2β cKO mice also have an increased thickness of optic tract (white arrows). (**P**) Dorsolateral to ventromedial length of the dLGN is significantly reduced at all ages *** (SEM) $p<0.005$, n = 3 Student's t-test. (**Q**) Medial to lateral width of the dLGN shows significant increase at all ages (SEM) $p<0.005$, n = 3 Student's t-test. (**R**) Thickness of optic tract is significantly larger at P7 (SEM) $p<0.01$ and adult (SEM) $p<0.005$ Tra2β mutant mouse, n = 3 Student's t-test. A-B Bar, 2.5mm; C-D Bar, 200μm; E-F Bar, 500μm; G-H Bar, 200μm; I-N Bar, 100μm.

Table 1:	**Ventromedial-Dorsolateral (μm)**			**Medial-Lateral (μm)**			**Optic tract thickness (μm)**		
Age	P2	P7	Adult	P2	P7	Adult	P2	P7	Adult
WT	945.4±9.4	1006±12.3	1400±25.8	166.1±3.5	342±13.7	342.1±3.7	53.2±2.4	42.8±1.6	72.8±3.3
Tra2β cKO	784.8±17.	808.9±12.3	886.4±27.1	206.5±6.8	418±5.7	523.3±24.3	59.7±4.3	69.8±3.8	168.1±11.2
WT	924.1±13.4								
Tbr1 KO	836.2±9.8								

We wanted to determine if the RGC axons that do project to the ventral dLGN in the Tra2β cKO are a subset of the image-forming RGCs that normally project there, or if the RGCs that project to the vLGN or IGL expand into the neighboring dLGN. To distinguish between these hypotheses, we crossed Tra2β cKO mice to an Isl2-GFP reporter line. This line expresses GFP in a subset of RGCs that send axonal

projections to the contralateral dLGN and SC, but not any other retinal recipient area (Triplett et al., 2014). We find that Isl2-GFP expressing axons send few, if any projections to the dLGN of adult Tra2β cKO mice (Fig. 9 A-D), but do target the SC normally (Fig. 9 E-J). We also find that Isl2-GFP labeled axons do not aberrantly project to any other retinal recipient areas (data not shown). These results suggest that the axons that target the ventral most portion of the dLGN in Tra2β cKO are likely to be from RGCs that normally target non-image forming areas, and that the RGC axons that normally target the dLGN now project solely to the SC.

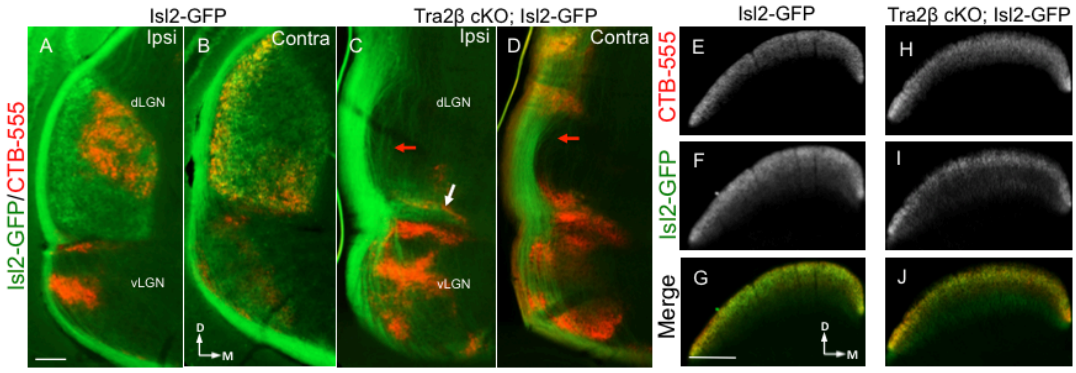

Figure. 9. **Image forming RGCs fail to properly target the dLGN.** 100µm coronal sections show the visual thalamus of an Isl2-GFP control mouse (note, all Isl2-GFP+ axons are contralateral projections (Triplett et al., 2014)), and Tra2β cKO; Isl2-GFP mouse with RGCs from one eye labeled with CTb-555 (red). Isl2-GFP+ (green) and CTB-labeled (red) axons in both ipsilateral (**A**) and contralateral (**B**) projections in the Isl2-GFP control mouse, GFP+ axons are restricted to the dLGN. Isl2-GFP+ (green) and CTB-labeled (red) axons in both ipsilateral (**C**) and contralateral (**D**) projections in the Tra2β cKO; Isl2-GFP mouse, GFP+ projections fail to terminate in dLGN except for a small horizontal fragment (white arrow) in the ipsilateral section, while contralateral dLGN does not contain any GFP+ terminations. The optic tract also shows increased thickness in mutant LGN (red arrows). Isl2-GFP control SC labeled with CTB-555 (**E**), Isl2-GFP (**F**), and merge (**G**) are similar to Tra2β cKO; Isl2-GFP SC innervations, CTB-555 (**H**), Isl2-GFP (**I**), and merge (**J**). A-D Bar, 100µm; E-J bar, 200µm

Morphogical and histological features of the Tra2β cKO retina and thalamus are similar to wild type.

Since we found that RGC axons no longer project to the region of the dLGN, we wanted to assess if developing without a cortex leads to a change in dLGN or retinal structure. Coronal sections through the thalamus stained with DAPI, NISSL, and cytochrome oxidase (CO) all showed that the dLGN can be morphologically identified, is maintained in the thalamus, and is metabolically active (Fig 10. A-H). We also found that ephrin-A5 and EphA7, genes known to be expressed in gradients in the vLGN and dLGN during development (Feldheim et al., 1998; Rashid et al., 2005), maintain their graded expression patterns in the Tra2β cKO mutants. (Fig. 10 I-L).

Retinal circuitry and RGC development remain unperturbed in Tra2β cKO mice. Using a lox-stop-lox; tdTomato Cre (tdT) reporter line we found very few tdT^+ cells (1.3 ± 0.1 SEM tdT^+ vs. 34.1 ± 3.4 SEM $DAPI^+$) per 100 μm of ganglion cell layer analyzed (data not shown). We also found no differences in the distribution or number of image-forming and non-image forming RGCs based on immunocytochemistry of retinas stained with Brn3a, a transcription factor expressed in image-forming RGCs (Quina et al., 2005) and Tbr2, a protein expressed selectively in RGCs that project to non-imaging forming areas (Sweeney et al., 2013) (Fig. 11 A-B, Table 2). The relative proportion of $Brn3a^+$ cells to $Tbr2^+$ cells was not significantly different (Table 2). General retinal structure and lamination patterns

were also normal in the mutant as assayed by DAPI and ChAT staining (Fig. 11 C-D).

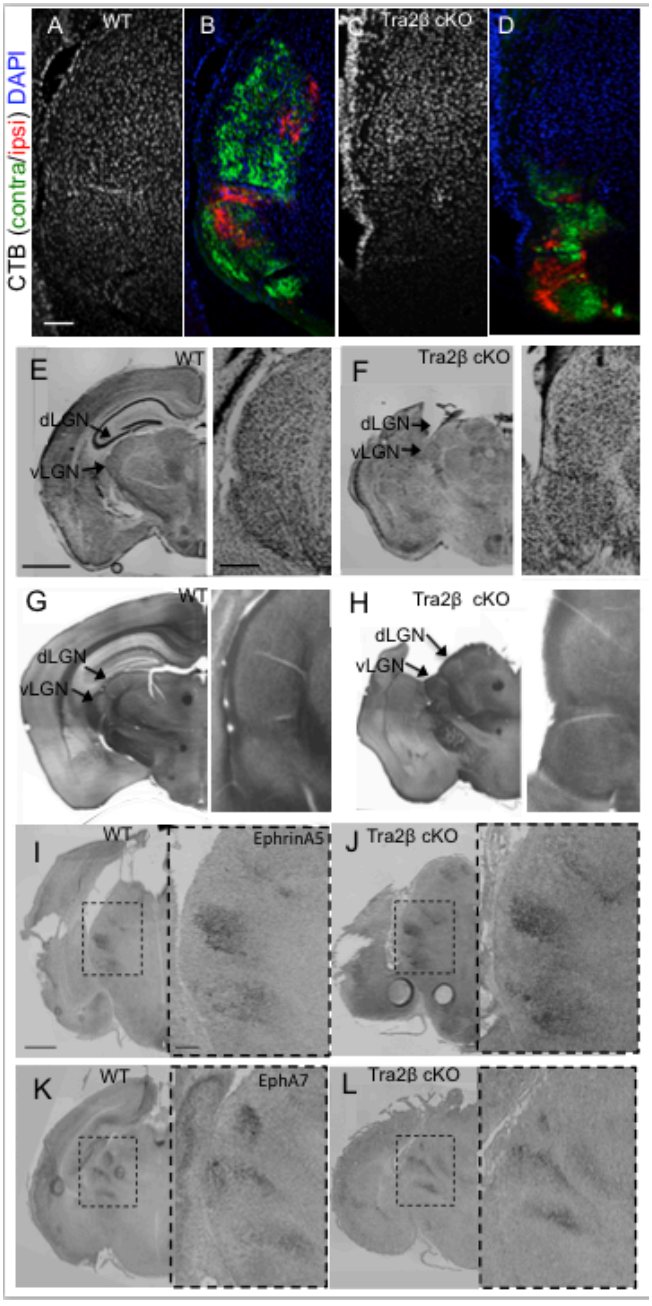

Figure. 10 **Tra2β cKO LGN tissue is similar to that of wild type controls. (A-D)** 20um coronal sections of adult animals stained with DAPI (blue) confirm the existence of cell nuclei in WT (**A**) and Tra2β cKO (**C**) visual thalamus, verified by labeling RGCs in right eye, CTb-488 (green) and left eye, CTb-555 (red) in WT (**B**)

and Tra2β cKO (**D**). (E-F) NISSL stained 50um sections of adult WT (**E**) and Tra2β cKO (**F**) (arrows indicate locations of dLGN and vLGN). (G-H) Cytochrome oxidase staining of 50um sections of adult WT (**G**) and Tra2β cKO (**H**) arrows indicate the dLGN and vLGN. (**I-L**) RNA in situ hybridization of coronal sections from P2 animals, dashed box indicates visual thalamus; Ephrin A5 expression in WT (**I**) and Tra2β cKO (**J**); EphA7 expression in WT (**K**) and Tra2β cKO (**L**) show similar patterns. Arrows indicate locations of dLGN and vLGN; zoom of original images inset. A-D bar, 100µm; E-H Bar, 1mm (200µm inset); I-L bar, 500µm (100µm inset)

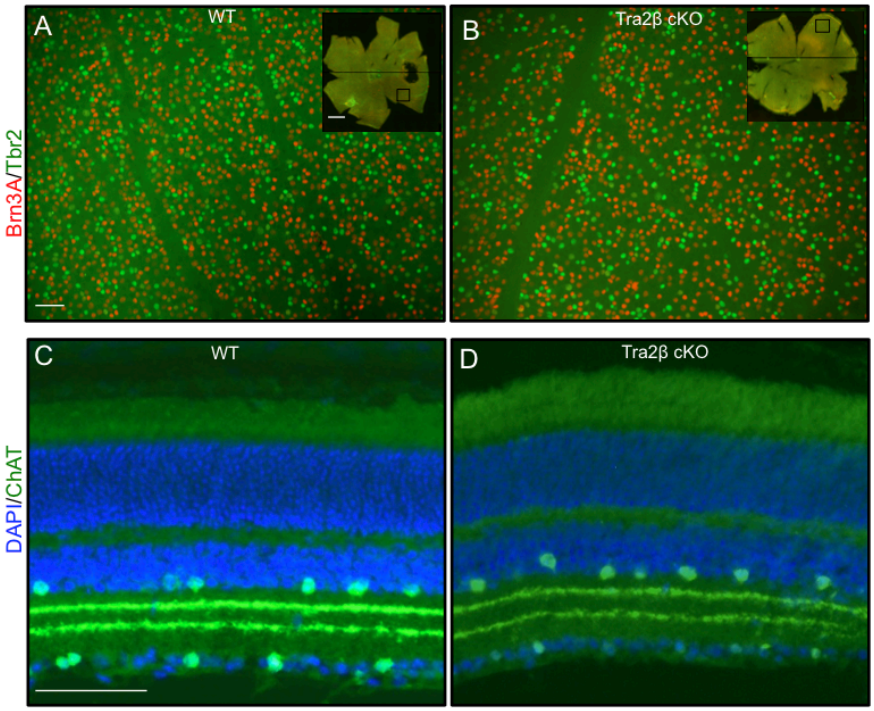

Figure. 11 **Tra2β cKO retinas have normal RGC populations and distributions. (A-B)** Flat mount adult WT (**A**) and Tra2β cKO (**B**) retinas ganglion cell layer up immunostained for the image-forming RGC marker Brn3A (red) and the non-image forming RGCs marker Tbr2 (green). Total number of Brn3A+ and Tbr2+ cells is not significantly different between WT and mutant, n=7. (**C-D**) 20um retina sections of WT (**C**) and Tra2β cKO (**D**) with placed and displaced amacrine cells labeled with ChAT (green) and DAPI (blue). The patterns of amacrine cells as well as their dendritic morphology were indistinguishable between mutants and controls. A-B Bar, inset 100µm, large 20µm; D-E Bar, 50µm

Table 2:	Brn3A+ cells/mm^2	Tbr2+ cells/mm^2	Brn3A+/Tbr2+ ratio
WT	13200±1452	4297±540	3.12/1
Tra2β cKO	15209±574	5292±309	2.91/1

Layer 6 cortical inputs to the dLGN are required for proper retinogeniculate targeting.

One major difference between the dLGN and the other retinal recipient areas is that the dLGN receives cortical inputs from layer 6 rather than layer 5. To determine if these layer 6 inputs are required for retinogeniculate targeting, we traced the retinal projections in Tbr1 null (Tbr1 KO) mice (Bulfone et al., 1998); the layer 6 cortical neurons in Tbr1 KO mice take on the fate of layer 5 neurons, as assayed by their expression of cortical layer 5 and layer 6 markers, cell morphology, and the fact that their axons fail to project to thalamic nuclei and instead project to the spinal tract or SC (Hevner et al., 2001; McKenna et al., 2012). Tbr1 KO mice die at early post-natal ages, but we were able to anterograde label RGC axon projections at birth and analyze their projection patterns at P2. Similar to the Tra2β cKO mice, RGC axons from Tbr1 KO mice exhibit defects in targeting the dorsal dLGN (Fig 12. A-B, Table 1). These data suggest that innervation of the visual thalamus by axons from cortical layer 6 during development is necessary for image forming RGCs to properly target

and/or terminate within the dLGN.

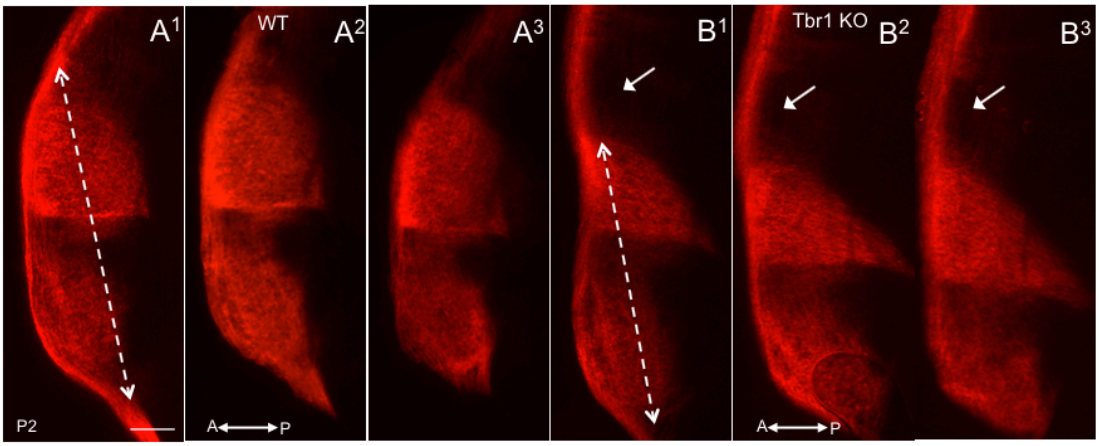

Figure. 12 **Image forming RGCs fail to properly target the dLGN of Tbr1 KO animals. (A-B)** Three serial sections of WT control mice (**A**$^{1\text{-}3}$) and Tbr1 KO (**B**$^{1\text{-}3}$), that have had their RGC axons labeled with CTb-555 (red). Distance of RGC innervation within LGN in control is significantly longer than mutant, leaving a space within dLGN lacking innervation (white arrows). A-B Bar, 100µm. A=anterior, P=posterior.

SC neurons in Tra2β cKO mutants have altered receptive field properties.

While RGCs can still project to the SC in mice that developed without a cortex, many studies have suggested that the cortical inputs to the SC participate in shaping the receptive field properties of a collicular neuron (Wang et al., 2010; Wang and Burkhalter, 2013; Zhao et al., 2014). We measured the visual response properties of SC neurons in Tra2β cKO and control mice in response to patterned stimuli. We used 2-shank, 64 or 128 channel silicon probes in the SC to record the visual response properties of SC neurons in awake mice that are head-fixed on a freely-floating Styrofoam ball used as a spherical treadmill while viewing a computer monitor (Fig. 13 A-B) (Dombeck et al., 2007; Harvey et al., 2009; Niell and Stryker, 2010). We displayed a number of stimuli, including a flashing spot stimulus (Wang et al., 2010),

a drifting sinusoidal gratings stimulus (Niell and Stryker, 2008), and a white noise stimulus (Chichilnisky, 2001). We found that many visual response properties were similar in the two sets of mice. Using the stationary spot stimulus we found that both WT and Tra2β cKO contained ON, OFF, and ON-OFF responses with no difference in RF size between WT and mutant (Fig. 13 C). However, we did find a change in the proportions of these cell types; the mutant shows a decrease in the number of ON-OFF cells and an increase in OFF cells compared to wild type, although this change is not highly significant (Fig. 13 D). Using a moving bar stimulus we found that both WT and mutant have similar proportions of direction selective and orientation selective SC neurons (Fig. 13 F-H). Interestingly, compared to WT, neurons in the Tra2β cKO mutant SC do not respond strongly to a white noise stimulus (Fig. 13 E).

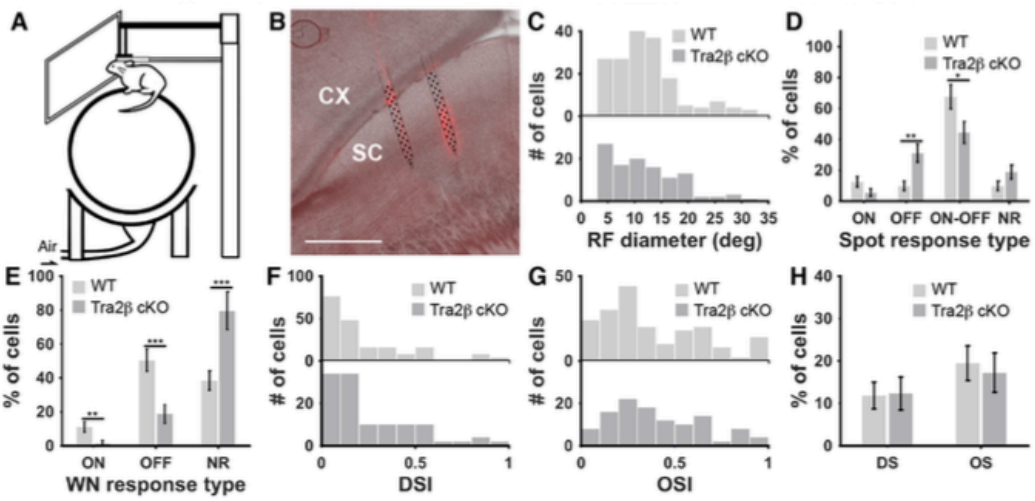

Figure. 13 **Significant changes were observed in flashing spot and white noise responses, but not in direction and orientation selectivity.**
(**A**) Schematic of the experimental setup for silicon probe electrophysiology. A mouse was freely behaving on a floating spherical treadmill during a recording session, while it was watching visual stimuli on the screen to its right. (**B**) Cryostat sagittal section showing DiI traces indicating location of inserted probe (red), schematic of the 64-channel probe is shown in black. (**C**) Histograms indicating

receptive field (RF) diameters of cells as measured in flashing spot responses. There were no significant differences between wildtype and Tra2β cKO distributions (Kolmogorov-Smirnov (KS) test, $p>0.05$). (**D**) Percentage of the ON, OFF, ON/OFF, and non-responsive (NR) neurons in response to the flashing spot stimulus. Error bars represent standard deviations. Significant increase of OFF cells, and significant decrease of ON/OFF cells were observed in Tra2β cKO mice. (** $p<0.01$ and ** $p<0.05$, respectively). (**E**) Percentage of the ON, OFF, NR cells in response to the white noise stimulus. Significant decreases were observed in both ON and OFF cells (** $p<0.01$ and *** $p<0.005$, respectively), resulting in increase of NR cells (*** $p<0.005$). (**F-G**) Histograms of DSI and OSI of cells measured in drifting sinusoidal grating stimulus. There were no significant differences between wildtype and Tra2β distributions (KS test, $p>0.05$). (**H**) Percentage of the OS cells and DS cells. There were no significant differences between WT and Tra2β cKO ($p>0.05$).

Tra2β cKO animals have normal non-image forming visual functions

Does developing without a cortex have an impact on visually-evoked behaviors? We tested the Tra2β cKO mice on a number of visually dependent tasks that are thought to use distinct retinal circuits. Consistent with normal innervation of the OPN and SCN, Tra2β cKO mutants display normal performance on behaviors that rely on non-image forming circuits, including the pupillary light reflex and circadian day/night activity cycles (Trejo and Cicerone, 1984; Chen et al., 2011; Hattar et al., 2002; Morin et al., 2006). To test the pupillary light reflex, mice were adapted to dark conditions and then exposed to 172 mW/cm2 (1%) and 2.9 mW/cm2 (5%) of light in the contralateral eye and the amount of total pupillary constriction was calculated. At 5% of light, the percentage of pupil constriction was not significantly different between Tra2β cKO and WT mice (mutant 79.08% ± 2.77 SEM; n=11; wild type 80.64% ± 1.8 SEM; n=10, $p > 0.05$, Student's t test) (Fig. 16 A-D, G). Similarly, the percentage of pupil constriction was not significantly different between Tra2β cKO

and WT mice at 1% of light (mutant 62.61% ± 3.67 SEM; n=12; wild type 60.54% ± 3.98 SEM; n=11, $p > 0.05$, Student's t test) (Fig. 14 A-B, E-F, G).

To test whether Tra2β cKO animals have normal day/night activity cycles, Tra2β cKO and WT mice were individually housed in cages that monitor activity by recording infrared beam breaks. Beam breaks were measured for 60 hours, which included 3 alternating 12-hour light/dark cycles. Tra2β cKO animals were significantly more active compared to WT animals during both the light (mutant 335 ± 76 SEM; n=12; wild type 223 ± 30 SEM; n=12, $p < 0.05$, Student's t test) and dark cycles (mutant 1254 ±160 SEM; n=12; wild type 721 ± 68 SEM; n=12, $p < 0.005$, Student's t test) (Fig. 14 H). Circadian rhythms in mice, which manifest as increased activity at night compared to the day, were apparent in both Tra2β cKO ($p < 0.005$, Student's t test) and wild type controls ($p < 0.005$, Student's t test). Taken together these data indicate that not only are the SCN and OPN innervated (Fig. 8 D, F) in Tra2β cKO animals the associated behaviors are preserved.

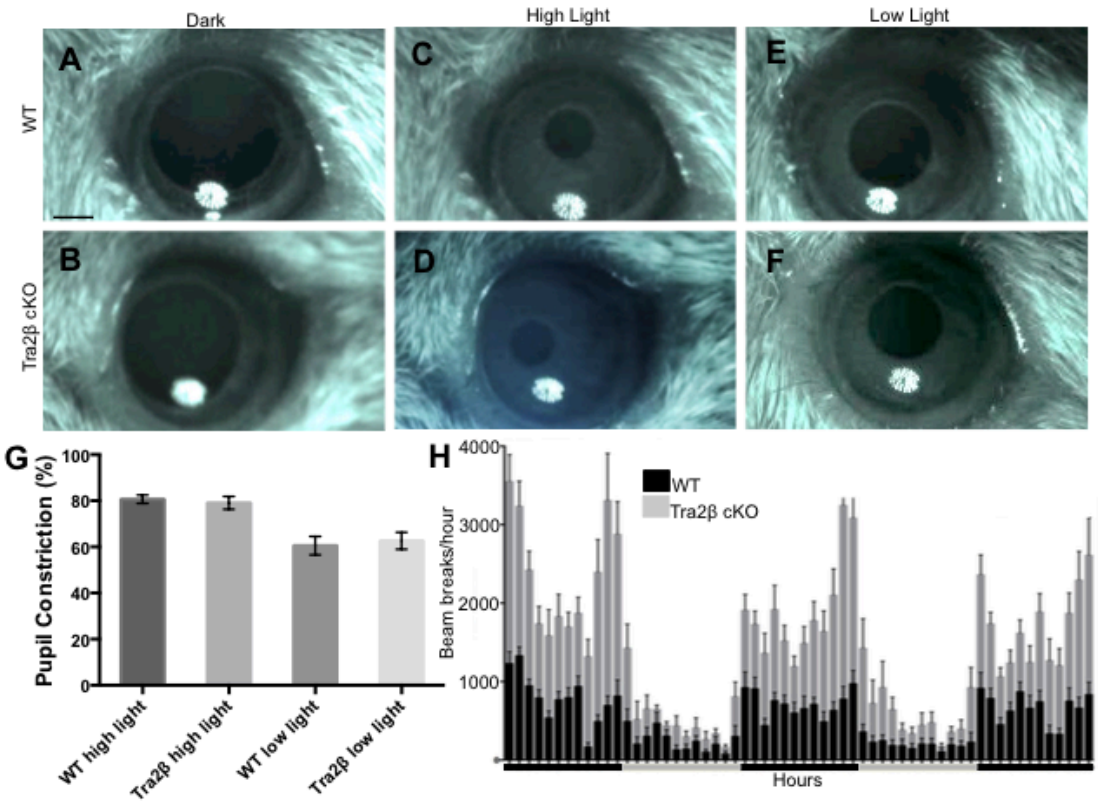

Figure. 14 **Pupillary light reflex and circadian rhythms are normal in Tra2β cKO animals. (A-F)** Adult control and Tra2β cKO mice were dark adapted for 1 minute (**A**,**B**) and then exposed to either high (2.9 mW/cm^2) (**C,D**) or low (172 mW/cm^2) (**E,F**) light intensity presented for 30 seconds to the contralateral eye, images were captured with an infrared camera. (**G**) Graph showing the percent pupil constriction in Tra2β cKO and control mice ($n \geq 10$ each), there is no significant difference at either light intensity ($p > 0.05$, Student's t-test). (**H**) The number of ambulatory beam breaks is shown in one-hour intervals across 60 hours of alternating 12-hour dark cycles (black bar) and 12-hour light cycles (gray bar). Wild type animals, black columns and Tra2β cKO animals, gray columns, error bars (SEM). A-F Bar, 500μm

Tra2β cKO mice can perform complex visual tasks

We assessed performance of Tra2β cKO mice on two complex behavioral tasks (cued Pavlovian fear conditioning and cued Morris Water Maze) to determine the ability of Tra2β cKO mice to use visual perception to guide behavior.

In the Pavlovian Fear Conditioning task, we tested whether Tra2β cKO mice could learn to associate a flashing light (cue) with an aversive stimulus (foot shocks). Increased freezing is indicative of a mouse's adaptive response to fear. Freezing upon presentation of the flashing light 24 hours after training indicates functional vision and recognition of the cue. Male and female Tra2β cKO and WT animals were conditioned using 10 light/shock pairings (see materials and methods). The conditioned mice were placed into a novel context 24 hours after training; time spent motionless was measured both before and during presentation of the cue (flashing light; Fig. 15 A). WT mice exhibited a significant increase in time spent freezing after the onset of the flashing light (before: 6.42 ± 2.53 sec vs. after: 24.8 ± 5.42 SEM; n=8 $p < 0.001$, Student's t test). Tra2β cKO also showed a significant increase in time spent freezing after the onset of the flashing light (before: 5.98 ± 2.69 sec. vs. after: 14 ± 3.39 SEM; n=12, $p < 0.005$, Student's t test). A control group was only exposed to the flashing light during day one acquisition and then again 24 hours later. Control mice showed no significant increase in time spent freezing after the onset of the flashing light (before: 5.07 ± 1.79 sec. vs. after: 2.09 ± 0.74 SEM; n=8, $p > 0.25$, Student's t test) suggesting that the significant increase in freezing apparent in both WT and Tra2β cKO is due to the association between visual perception of the flashing light and memory of the aversive stimulus (Fig. 15 B). These data are consistent with findings from Shang et al. (Science, 2015) who used an optogenetic approach with the parvalbumin-positive excitatory visual pathway in the SC to discover that this pathway was sufficient to drive a flight or flight response. These

data suggest that even in the absence of cortical development, Tra2B cKO animals can perceive a visual stimulus and correlate it to an aversive stimulus.

In the cued Morris Water Maze task, we assessed whether Tra2β cKO mice could use visual perception of a cue to guide movement to an escape platform (Prusky and Douglas, 2004) (Fig. 15 C). Time to locate an escape platform marked by a visual cue was measured in Tra2β cKO and WT animals across three consecutive days (Fig. 15 D). WT mice learned to use the visual cue to locate the escape platform as suggested by decreased time to reach the platform across the three days ($p < 0.001$, n=13, ANOVA). Time to reach the platform also significantly decreased in Tra2β cKO across the three days, suggesting that Tra2β cKO also learned to use the visual cue to locate the platform ($p < 0.03$, n=11, ANOVA) (Fig. 15 D). Although Tra2β cKO were able locate the escape platform using visual cues, time to locate the platform was significantly shorter in WT mice compared to Tra2β cKO mice ($p < 0.001$, ANOVA). Swim speed is not significantly different between WT and Tra2β cKO mice (WT: 1.01 ± 0.05 m/s; cKO: 0.99 ± 0.05 m/s; $p = 0.22$, ANOVA), which suggests that impaired performance on the task is not associated with an inability to swim.

During the spatial version of the Morris Water Maze task in which the platform is hidden, mice develop search strategies to locate the hidden platform (Vorhees and Williams, 2006). To rule out the possibility that Tra2β cKO mice were using strategies besides vision to locate the platform, the cue was removed from the platform on the last two trials on Day 3, and we compared the time to reach the

platform with and without the cue. Both WT and Tra2β cKO mice took significantly longer to find the escape platform after the cue was removed (WT: 12.37 ± 1.86 vs. 36.21 ± 4.17 seconds, $p < 0.001$, ANOVA; cKO: 22.68 ± 2.83 vs. 46.91 ± 3.79, $p < 0.001$, ANOVA) indicating that both WT and Tra2β cKO mice are significantly better when the cue is in place. These data suggest that perception of a visual cue is responsible for both WT and mutant animal's ability to locate the hidden platform. This test coupled with the fear-conditioning paradigm demonstrates that the Tra2β cKO animals, although lacking a visual cortex and the proper RGC innervation within the dLGN, have the ability to perceive light and perform complex visual tasks.

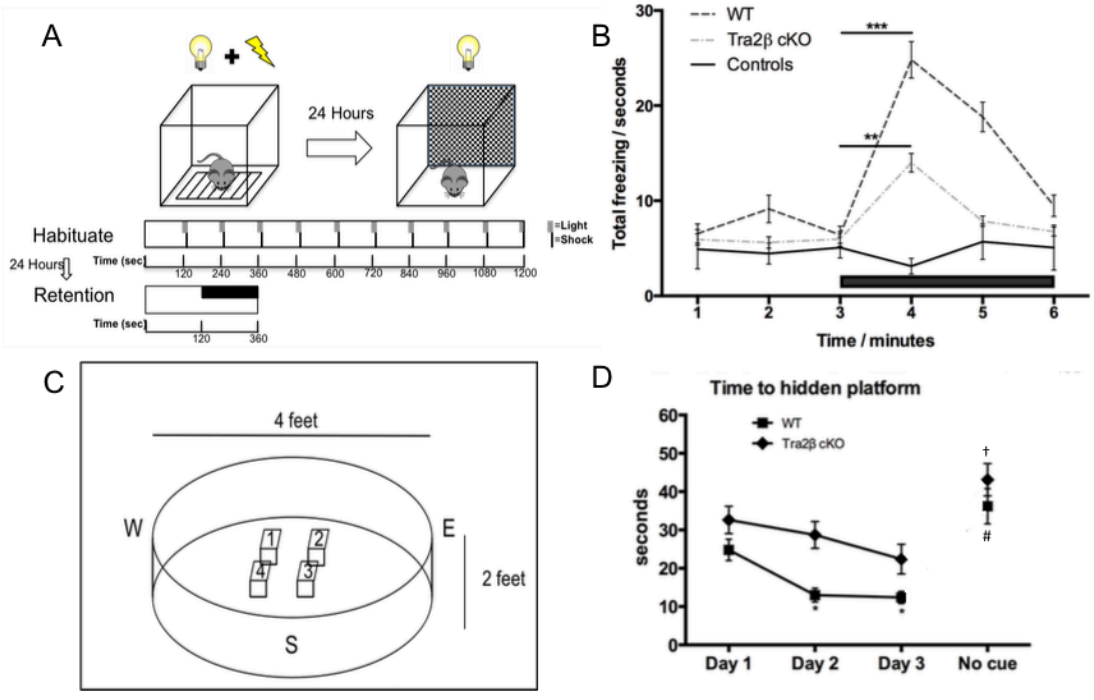

Figure. 15 **Tra2β animals perceive light and can navigate a complex task.** (**A**) Pavlovian fear conditioning design, animals are conditioned on day one by pairing an unconditioned stimulus (shock) with a conditioned stimulus (flashing light). On day two, animals are placed in a novel context, 180 seconds of darkness is followed by 180 seconds of flashing light (black bar). (**B**) There is a significant increase in the

amount of freezing in wild type (black dashed line) and Tra2β cKO (gray dashed line) mice in the 60 seconds after the onset of flashing light compared to the previous 60 seconds of darkness, control (non-conditioned) animals (black line) do not have a significant response after the onset of light. (**C**) Schematic of water maze design indicates four stage positions and three entry points. Day one and two consist of 4 trials each day, the platform is labeled with a visual cue. Day three, the first two trials the stage is labeled with a visual cue and the next two trials the cue is removed. (**D**) Tra2β cKO and WT control animals find the hidden platform significantly better each day and when the cue is removed the animals find the cue significantly worse. * $p < 0.001$ vs. WT Day 1; # $p < 0.05$ vs. WT Day 3; † $p < 0.05$ vs. cKO Day 3

Discussion

The visual cortex receives visual information from the dLGN and feeds back to many subcortical thalamic and brainstem retinorecipient areas to modulate visual responses and behaviors. Here we describe a novel function of the cortex during development - that it is required for the ability of image-forming RGC axons to target to the dLGN. The dLGN is unique among RGC targets; it is the only retinorecipient area that sends projections directly to the cortex and is the only area that receives descending projections from layer 6 cortical neurons. This suggests that the axons from these layer 6 neurons are required for dLGN targeting. Consistent with this, a Tbr1 mutant mouse that has fewer layer 6 inputs to the dLGN also lacks the normal amount of retinal axons in the dLGN. Using physiological recording methods we find that the loss of cortex does indeed affect the receptive field properties of SC neurons, most dramatically in their ability to respond to white noise stimuli. We also find that the development of a cortex is not required for the ability of mice to execute a number of visually dependent behavioral tasks.

Cortical input from layer 6 neurons is required for image-forming RGC axons to target the dLGN.

We found that image-forming axons fail to project to the dLGN in both mice that develop without a visual cortex (Tra2β cKO) and mice that lack layer 6 projections to the thalamus (Tbr1 KO). This lack of targeting can be detected as early as P2 and is maintained into adulthood. We do not think that the targeting defect is due to the loss of RGCs or target cells in Tra2β cKO mice because we did not find a decrease of RGC numbers in the retina, nor did we detect patterning defects in the mutant retina or thalamus. We also found that Isl2-GFP RGC axons that normally project to the SC and dLGN now only target the SC and bypass the dLGN. Taken together, our work leads to the hypothesis that cortical layer 6 axons provide an activity or cue during development that is required for RGC axons to terminate and branch within the dLGN.

These findings are somewhat counterintuitive to the idea that RGC axons promote dLGN innervation by cortical layer 6 axons (Brooks et al., 2013). Fox, Guido, and colleagues used the Golli-τ-GFP mouse, which expresses GFP in layer 6 axons (Jacobs et al. 2007), to show that layer 6 axons initially pause at the medial shell of the dLGN at P2, begin to innervate the dLGN at P4, and fill the entire dLGN by P14. During this time, RGC axons innervate the dLGN. Removal of RGC inputs accelerates the timing of cortical innervation, as does the degradation of Aggrecan, a repulsive chondroitin sulfate proteoglycan expressed in early post-natal dLGN

(Seabrook et al., 2013; Brooks et al., 2013). These results suggest RGC innervation plays a critical role in the timing of cortical axon invasion into the dLGN. However, they do not predict that cortical axons would be required for retinal axons targeting the dLGN, because most of these axons are not in the dLGN at the time of targeting. To reconcile these differences we propose a model whereby the small amount of cortical fibers present in the dLGN at early postnatal stages when RGC axons converge, or factors secreted from the cortical axons located at the border of the medial thalamus, could be providing an activity used to promote RGC axon branching from the optic tract. This activity could be used to remove a repellent molecule found in the dLGN, similar to that proposed for Aggrecan, or be used to attract axons or promote selective adhesion as is proposed in non-image forming areas for Reelin (IGL targeting), contactin/APP (NOT targeting), and Sema6A/Npl (MTN targeting) (Su et al;. 2011; Osterhout et al., 2014; Sun et al., 2015). However, in each of the above instances, the targeting activity is located in the RGC axons and the target cells. Therefore, our work reveals a novel mechanism to deliver a target-matching cue through the axons of a third party.

Development of a cortex is required for the development of receptive field properties in the superior colliculus.

Neurons in the superficial SC receive inputs from both RGCs and layer 5 neurons in the visual cortex (Chandrasekaran et al., 2007; Drager and Hubel, 1975). SC neurons have many distinct visual response properties including ON, OFF, ON-

OFF, direction selective, and orientation selective visual responses (Wang et al., 2010). The contribution of layer 5 inputs to the receptive field properties of collicular neurons has been tested in animals that have had cortical ablations, cortical cooling, or light induced silencing with mixed results; some fail to show a large effect on the receptive field properties, while others only show that they participate in the gain of the responses (Ogasawara et al., 1984). These results can potentially be explained by the state of the animal, the severity of the lesion, or the visual stimulus presented (Zhao et al., 2014). In each of these previous experiments the cortex was manipulated in the adult animal after the connectivity between the cortex and the SC had been established. Consistent with results from Zhao et al., in which optogenetics were used to silence V1 inputs to the SC (Zhao et al., 2014), we find that lack of a cortex during development has very little effect on the circuitry that creates On, Off, direction selective or orientation selective SC neurons that respond to spots or moving bar stimuli. However, we find a dramatic reduction in the number of neurons that respond to a white noise stimulus. White noise is different from a spot stimulus in that the whole visual field is illuminated while each pixel flickers between light and dark independent of other pixels. Therefore, cells that receive strong surround suppression do not respond well to this stimulus. Of the four cell types previously identified by Gale and Murphy, horizontal cells and stellate cells are less influenced by surround suppression than wide field and narrow field cells. A reduction in the number of SC cells and preserved response to local spot stimuli are suggestive of the loss of

response of these two cell types. Interestingly, they both project to the dLGN, which is developmentally compromised in Tra2β cKO mice (Gale and Murphy, 2014).

Visually evoked behaviors of Tra2β cKO mice remain intact

We found that developing without a cortex does not affect the ability of mice to respond to light, as assayed by their performance in 4 different tasks. We found that Tra2β cKO mice have a normal pupillary light reflex, have normal light-dark activity cycles, can associate a shock with a visual cue, and can find a hidden platform using a visual cue. The first three tasks are thought to involve RGC axonal input into the OPN, SCN, and SC respectively, and targeting RGCs to these areas remains normal in the Tra2β cKO (Trejo et al., 1984; Shang et al., 2015). Rodents with a bilateral V1 lesion have shown diminished acuity in the hidden platform task (Prusky and Douglas, 2004). Our results suggest that the visual system is plastic, and that developing without a cortex allows the subcortical visual circuitry to permit Tra2β cKO mutants to perceive a flashing light and locate a hidden platform. Therefore, the Tra2β cKO mouse may act like humans with bilateral V1 lesions; such people have the ability to detect and discriminate visual stimuli that they cannot consciously recognize (Stoerig and Cowey, 1997). Future studies aimed to characterize the visual acuity and perception of Tra2β cKO mice is needed to fully understand how the cortex, thalamus, and SC coordinate to achieve perception and behavior.

Conclusions

Cortical layer 6 is necessary for proper RGC axon targeting to dLGN

To better understand how billions of neurons in the human brain make trillions of connections it is first important to understand the basic underlying principles of how proper axonal connections are made in a stereotypic manner. There is building evidence that, receptor tyrosine kinases, cell adhesion molecules, and activity play an important role in producing appropriate connections within the mouse visual system. Sperry hypothesized that a molecular matching system in which target cells express a recognition molecule, which allows neurons to locate and synapse with their appropriate target, existed and this system is responsible for the precise wiring of the brain (Sperry, 1963). Indeed, all of the current molecular matching examples in the mouse visual system demonstrate that the target cell produces the molecule responsible for the appropriate recognition, or that activity in either the cell or the target is necessary for refinement but not location recognition (Pfeiffenberger et al., 2005; Inoue and Sanes, 1997; Su et al., 2011; Osterhout et al., 2015; Sun et al., 2015; Rossi et al., 2001; Dhande et al., 2011). My work has potentially uncovered a novel mechanism. One in which a third party axon, in this case cortical layer 6 output neurons, provides either an activity, a specific membrane bound molecule necessary for recognition or possibly a secreted signal responsible for RGCs to appropriately target the dorsal region of the mouse visual thalamus (figure 17).

Mutant mice lacking cortical layer 6 output neurons have the same loss of RGC input in the dLGN at early time points as mice that develop without a cortex.

This recapitulated phenotype bolsters the argument that cortical layer 6 neurons are necessary for the proper targeting of RGCs to the dLGN. RNA sequencing data of cortical tissue taken from animals that lack layer 6 neurons exists and it is possible that these data will yield candidates for future studies. Potential molecules of interest include neurotrophic factors and known axon guidance molecules. It will be interesting to see if likely candidates provide fruitful information.

Image forming and non-image forming behaviors exist in animals that develop without a cortex

It has been well established that specific non-image forming behaviors including the pupillary light reflex and circadian rhythms are reliant on the innervation of ipRGCs (Sweeney et al., 2014; Hattar et al., 2002). Labeling experiments have shown that cortical layer 5 output neurons innervate the OPN, the subcortical nuclei responsible for dictating the pupillary light reflex, what is not known is whether this innervation is critical for a functional reflex. My work indicates that a mouse that develops without a cortex indeed has a completely functional and normal pupillary light reflex in the absence of cortical layer 5 input. The SCN, necessary for proper sleep wake cycles in mammals, does not receive direct cortical innervation; it does however send information directly to the cortex as well as other subcortical nuclei (Saper et al., 2005). My work in animals that develop without a cortex indicates that direct RGC input into the SCN is sufficient to regulate sleep wake cycles as my experiments indicated a marked increase in activity during

times of darkness and decreased activity when light was present however, it seems that in the absence of cortical influence the animals are much more active during the night cycles. Elucidating the mechanism behind this increased activity will need further attention.

Multiple studies have attempted to understand the necessity for the visual cortex (V1) during active vision. Lawrence Weiskrantz has investigated people with the ability to see after a lesion destroys their V1, he even coined the term *blindsight* to identify this phenomenon. He found that in patients with bilateral V1 lesions the individuals could still perceive their surroundings (Weisenkrantz, 2004). While the phenomenon of *blindsight* has been studied at length in humans, more recently it has been investigated in multiple animal models. Studies in mice utilizing channel rhodopsin to activate inhibitory neurons within the V1 suggest the need for V1 in recognition and perception of the visual scene (Glickfeld et al., 2013). Another study suggests that complete ablation of V1 affects image, motion and orientation discrimination but the ability to perceive approaching targets is intact (Petruno et al., 2013). While others argue that lack of V1 only modestly changes visual acuity (Dean et al, 1981). In all of these cases, whether by cortical lesion, optogenetic silencing, or surgical removal of V1 the original circuitry is allowed to develop normally and is altered later in life.

My thesis work allowed me to investigate how loss of V1 at early stages affects vision and circumvents many specific problems with previous investigations including: incomplete removal of V1 tissue in experiments where lesions were

utilized and incomplete coverage and expression when viral expression methods were performed. While I only used two basic vision paradigms in my thesis work, I discovered that mice that develop without a cortex can perceive light and use this perceptive ability to locate a hidden platform marked with a visual cue. These data only indicate that the mice can perceive light, the next set of questions will hopefully address whether the animals have the ability to discriminate what they see.

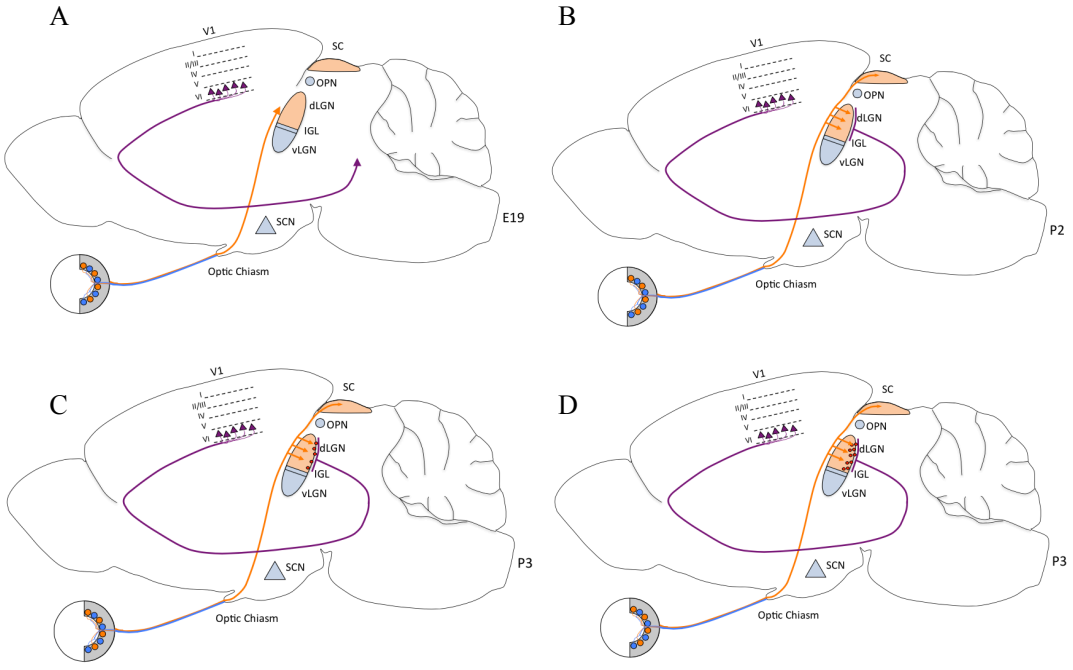

Figure 16. **A proposed model of my work: Cortical layer 6 neurons provide a membrane bound or secreted molecule, or an activity, for the proper targeting of RGCs to the dLGN:** (**A**) RGC axons are located near the dLGN by embryonic day 19 (E19) (orange) while output neurons from cortical layer 6 are entering the thalamus (purple). (**B**) At postnatal day 2 (P2) RGC axons have correctly targeted the dLGN (orange) and cortical layer 6 neurons are waiting at the medial shell (purple). (**C-D**) By P3 cortical neurons are potentially supplying a factor necessary for continued synapse formation within the dLGN.

Bibliography

Amir, S., & Stewart, J. (1996). Resetting of the circadian clock by a conditioned stimulus. *Nature*, *379*(6565), 542-545.

Bourassa, J., & Deschênes, M. (1995). Corticothalamic projections from the primary visual cortex in rats: a single fiber study using biocytin as an anterograde tracer. *Neuroscience*, *66*(2), 253-263.

Brooks, J. M., Su, J., Levy, C., Wang, J. S., Seabrook, T. A., Guido, W., & Fox, M. A. (2013). A molecular mechanism regulating the timing of corticogeniculate innervation. *Cell reports*, *5*(3), 573-581.

Buchmann, A., Dentico, D., Peterson, M. J., Riedner, B. A., Sarasso, S., Massimini, M., Tononi, G. & Ferrarelli, F. (2014). Reduced mediodorsal thalamic volume and prefrontal cortical spindle activity in schizophrenia. *Neuroimage*, *102*, 540-547.

Bulfone, A., Wang, F., Hevner, R., Anderson, S., Cutforth, T., Chen, S., Meneses, J., Pedersen, R., Axel, R. & Rubenstein, J. L. (1998). An olfactory sensory map develops in the absence of normal projection neurons or GABAergic interneurons. *Neuron*, *21*(6), 1273-1282.

Chandrasekaran, A. R., Shah, R. D., & Crair, M. C. (2007). Developmental homeostasis of mouse retinocollicular synapses. *The Journal of neuroscience*, *27*(7), 1746-1755.

Chang, Y. S., Owen, J. P., Desai, S. S., Hill, S. S., Arnett, A. B., Harris, J., Marco, E. & Mukherjee, P. (2014). Autism and sensory processing disorders: shared white matter disruption in sensory pathways but divergent connectivity in social-emotional pathways.

Chen, S. K., Badea, T. C., & Hattar, S. (2011). Photoentrainment and pupillary light reflex are mediated by distinct populations of ipRGCs. *Nature*, *476*(7358), 92-95.

Chichilnisky, E. J. (2001). A simple white noise analysis of neuronal light responses. *Network: Computation in Neural Systems*, *12*(2), 199-213.

Clandinin, T. R., & Feldheim, D. A. (2009). Making a visual map: mechanisms and molecules. *Current opinion in neurobiology*, *19*(2), 174-180.

Cosenza, R. M., & Moore, R. Y. (1984). Afferent connections of the ventral lateral geniculate nucleus in the rat: an HRP study. *Brain research*, *310*(2), 367-370.

Delogu, A., Sellers, K., Zagoraiou, L., Bocianowska-Zbrog, A., Mandal, S., Guimera, J. & Lumsden, A. (2012). Subcortical visual shell nuclei targeted by ipRGCs develop from a Sox14+-GABAergic progenitor and require Sox14 to regulate daily activity rhythms. *Neuron*, *75*(4), 648-662.

Dhande, O. S., Hua, E. W., Guh, E., Yeh, J., Bhatt, S., Zhang, Y., ... & Crair, M. C. (2011). Development of single retinofugal axon arbors in normal and β2 knock-out mice. *The Journal of Neuroscience*, *31*(9), 3384-3399.

Dhande, O. S., & Huberman, A. D. (2014). Retinal ganglion cell maps in the brain: implications for visual processing. *Current opinion in neurobiology*, *24*, 133-142.

Distler, C., & Hoffmann, K. P. (2011). Visual pathway for the optokinetic reflex in infant macaque monkeys. *The Journal of Neuroscience*, *31*(48), 17659-17668.

Dombeck, D. A., Khabbaz, A. N., Collman, F., Adelman, T. L., & Tank, D. W. (2007). Imaging large-scale neural activity with cellular resolution in awake, mobile mice. *Neuron*, *56*(1), 43-57.

Drager, U. C., & Hubel, D. H. (1975). Responses to visual stimulation and relationship between visual, auditory, and somatosensory inputs in mouse superior colliculus. *Journal of Neurophysiology*, *38*(3), 690-713.

Du, J., Blanche, T. J., Harrison, R. R., Lester, H. A., & Masmanidis, S. C. (2011). Multiplexed, high density electrophysiology with nanofabricated neural probes. *PLoS One*, *6*(10), e26204.

Erisir, A., Van Horn, S. C., & Sherman, S. M. (1997). Relative numbers of cortical and brainstem inputs to the lateral geniculate nucleus. *Proceedings of the National Academy of Sciences of the United States of America*, 1517-1520.

Feldheim, D. A., Vanderhaeghen, P., Hansen, M. J., Frisén, J., Lu, Q., Barbacid, M., & Flanagan, J. G. (1998). Topographic guidance labels in a sensory projection to the forebrain. *Neuron*, *21*(6), 1303-1313.

Feldheim, D. A., Kim, Y. I., Bergemann, A. D., Frisén, J., Barbacid, M., & Flanagan, J. G. (2000). Genetic analysis of ephrin-A2 and ephrin-A5 shows their requirement in multiple aspects of retinocollicular mapping. *Neuron*, *25*(3), 563-574.

Fraley, C., & Raftery, A. E. (1998). How many clusters? Which clustering method? Answers via model-based cluster analysis. *The computer journal*, *41*(8), 578-588.

Gale, S. D., & Murphy, G. J. (2014). Distinct representation and distribution of visual information by specific cell types in mouse superficial superior colliculus. *The Journal of Neuroscience*, *34*(40), 13458-13471.

Gorski, J. A., Talley, T., Qiu, M., Puelles, L., Rubenstein, J. L., & Jones, K. R. (2002). Cortical excitatory neurons and glia, but not GABAergic neurons, are produced in the Emx1-expressing lineage. *The Journal of neuroscience*, *22*(15), 6309-6314.

Hattar, S., Liao, H. W., Takao, M., Berson, D. M., & Yau, K. W. (2002). Melanopsin-containing retinal ganglion cells: architecture, projections, and intrinsic photosensitivity. *Science*, *295*(5557), 1065-1070.

Harrington, M. E. (1997). The ventral lateral geniculate nucleus and the intergeniculate leaflet: interrelated structures in the visual and circadian systems. *Neuroscience & Biobehavioral Reviews*, *21*(5), 705-727.

Harvey, C. D., Collman, F., Dombeck, D. A., & Tank, D. W. (2009). Intracellular dynamics of hippocampal place cells during virtual navigation. *Nature*, *461*(7266), 941-946.

Hevner, R. F., Shi, L., Justice, N., Hsueh, Y. P., Sheng, M., Smiga, S., Bulfone, A., Goffinet, A. M., Campagnoni, A.T. & Rubenstein, J. L. (2001). Tbr1 regulates differentiation of the preplate and layer 6. *Neuron*, *29*(2), 353-366.

Hildebrand, G. D., & Fielder, A. R. (2011). Anatomy and Physiology of the Retina. In *Pediatric retina* (pp. 39-65). Springer Berlin Heidelberg.

Huberman, A. D., Manu, M., Koch, S. M., Susman, M. W., Lutz, A. B., Ullian, E. M. & Barres, B. A. (2008). Architecture and activity-mediated refinement of axonal projections from a mosaic of genetically identified retinal ganglion cells. *Neuron*, *59*(3), 425-438.

Huberman, A. D., Wei, W., Elstrott, J., Stafford, B. K., Feller, M. B., & Barres, B. A. (2009). Genetic identification of an On-Off direction-selective retinal ganglion cell subtype reveals a layer-specific subcortical map of posterior motion. *Neuron*, *62*(3), 327-334.

Inoue, A., & Sanes, J. R. (1997). Lamina-specific connectivity in the brain: regulation by N-cadherin, neurotrophins, and glycoconjugates. *Science*, *276*(5317), 1428-1431.

Jacobs, E. C., Campagnoni, C., Kampf, K., Reyes, S. D., Kalra, V., Handley, V., Xie, Y., Hong-Hu, Y., Spreur, V., Fisher, R.S., & Campagnoni, A. T. (2007).

Visualization of corticofugal projections during early cortical development in a τ-GFP-transgenic mouse. *European Journal of Neuroscience*, *25*(1), 17-30.

Jaubert-miazza, L., Green, E., Lo, F. S., Bui, K., Mills, J., & Guido, W. (2005). Structural and functional composition of the developing retinogeniculate pathway in the mouse. *Visual neuroscience*, *22*(05), 661-676**.**

Kádár, A., Wittmann, G., Liposits, Z., & Fekete, C. (2009). Improved method for combination of immunocytochemistry and Nissl staining. *Journal of neuroscience methods*, *184*(1), 115-118.

Kana, R. K., Libero, L. E., & Moore, M. S. (2011). Disrupted cortical connectivity theory as an explanatory model for autism spectrum disorders. *Physics of life reviews*, *8*(4), 410-437.

Kay, J. N., De la Huerta, I., Kim, I. J., Zhang, Y., Yamagata, M., Chu, M. W. & Sanes, J. R. (2011). Retinal ganglion cells with distinct directional preferences differ in molecular identity, structure, and central projections. *The Journal of Neuroscience*, *31*(21), 7753-7762

Kim, I. J., Zhang, Y., Yamagata, M., Meister, M., & Sanes, J. R. (2008). Molecular identification of a retinal cell type that responds to upward motion. *Nature*, *452*(7186), 478-482.

Kim, I. J., Zhang, Y., Meister, M., & Sanes, J. R. (2010). Laminar restriction of retinal ganglion cell dendrites and axons: subtype-specific developmental patterns revealed with transgenic markers. *The Journal of Neuroscience*, *30*(4), 1452-1462.

Krahe, T. E., El-Danaf, R. N., Dilger, E. K., Henderson, S. C., & Guido, W. (2011). Morphologically distinct classes of relay cells exhibit regional preferences in the dorsal lateral geniculate nucleus of the mouse. *The Journal of Neuroscience*, *31*(48), 17437-17448.

Litke, A. M., Bezayiff, N., Chichilnisky, E. J., Cunningham, W., Dabrowski, W., Grillo, A. A., Grivich, M., Grybos, P., Hottowy, P., Kachiguine, R.S., Kalmar, S., Mathieson, K., Petrusca, D., Rahman, M. & Sher, A. (2004). What does the eye tell the brain?: Development of a system for the large-scale recording of retinal output activity. *Nuclear Science, IEEE Transactions on*, *51*(4), 1434-1440.

Masland, R. H. (2012). The neuronal organization of the retina. *Neuron*, *76*(2), 266-280.

May, P. J. (2006). The mammalian superior colliculus: laminar structure and connections. *Progress in brain research*, *151*, 321-378**.**

McKenna, W. L., Betancourt, J., Larkin, K. A., Abrams, B., Guo, C., Rubenstein, J. L., & Chen, B. (2011). Tbr1 and Fezf2 regulate alternate corticofugal neuronal identities during neocortical development. *The Journal of Neuroscience*, *31*(2), 549-564.

Mende, Y., Jakubik, M., Riessland, M., Schoenen, F., Roßbach, K., Kleinridders, A., Köhler, C., Buch, T., & Wirth, B. (2010). Deficiency of the splicing factor Sfrs10 results in early embryonic lethality in mice and has no impact on full-length SMN/Smn splicing. *Human molecular genetics*, *19*(11), 2154-2167.

Morin, L. P., Blanchard, J. H., & Provencio, I. (2003). Retinal ganglion cell projections to the hamster suprachiasmatic nucleus, intergeniculate leaflet, and visual midbrain: bifurcation and melanopsin immunoreactivity. *Journal of Comparative Neurology*, *465*(3), 401-416

Morin, L. P., & Allen, C. N. (2006). The circadian visual system, 2005. *Brain research reviews*, *51*(1), 1-60

Morin, L. P., & Studholme, K. M. (2014). Retinofugal projections in the mouse. *Journal of Comparative Neurology*, *522*(16), 3733-3753.

Niell, C. M., & Stryker, M. P. (2008). Highly selective receptive fields in mouse visual cortex. *The Journal of neuroscience*, *28*(30), 7520-7536.

Niell, C. M., & Stryker, M. P. (2010). Modulation of visual responses by behavioral state in mouse visual cortex. *Neuron*, *65*(4), 472-479.

Ogasawara, K., McHaffie, J. G., & Stein, B. E. (1984). Two visual corticotectal systems in cat. *Journal of Neurophysiology*, *52*(6), 1226-1245.

Osterhout, J. A., Josten, N., Yamada, J., Pan, F., Wu, S. W., Nguyen, P. L., Panagiotakos, G. & Huberman, A. D. (2011). Cadherin-6 mediates axon-target matching in a non-image-forming visual circuit. *Neuron*, *71*(4), 632-639.

Osterhout, J. A., Stafford, B. K., Nguyen, P. L., Yoshihara, Y., & Huberman, A. D. (2015). Contactin-4 Mediates Axon-Target Specificity and Functional Development of the Accessory Optic System. *Neuron*, *86*(4), 985-999.

Panda, S., Provencio, I., Tu, D. C., Pires, S. S., Rollag, M. D., Castrucci, A. M. & Hogenesch, J. B. (2003). Melanopsin is required for non-image-forming photic responses in blind mice. *Science*, *301*(5632), 525-527.

Phillips, R. G., & LeDoux, J. E. (1992). Differential contribution of amygdala and hippocampus to cued and contextual fear conditioning. *Behavioral neuroscience*, *106*(2), 274

Pfeiffenberger, C., Cutforth, T., Woods, G., Yamada, J., Rentería, R. C., Copenhagen, D. R., Flanigan, J. G., & Feldheim, D. A. (2005). Ephrin-As and neural activity are required for eye-specific patterning during retinogeniculate mapping. *Nature neuroscience*, *8*(8), 1022-1027.

Piscopo, D. M., El-Danaf, R. N., Huberman, A. D., & Niell, C. M. (2013). Diverse visual features encoded in mouse lateral geniculate nucleus. *The Journal of neuroscience*, *33*(11), 4642-4656.

Prusky, G. T., & Douglas, R. M. (2004). Characterization of mouse cortical spatial vision. *Vision research*, *44*(28), 3411-3418.

Quina, L. A., Pak, W., Lanier, J., Banwait, P., Gratwick, K., Liu, Y., Velasquez, T., O'Leary, D., Goulding, M. & Turner, E. E. (2005). Brn3a-expressing retinal ganglion cells project specifically to thalamocortical and collicular visual pathways. *The Journal of neuroscience*, *25*(50), 11595-11604.

Rashid, T., Upton, A. L., Blentic, A., Ciossek, T., Knöll, B., Thompson, I. D., & Drescher, U. (2005). Opposing gradients of ephrin-As and EphA7 in the superior colliculus are essential for topographic mapping in the mammalian visual system. *Neuron*, *47*(1), 57-69.

Rivlin-Etzion, M., Zhou, K., Wei, W., Elstrott, J., Nguyen, P. L., Barres, B. A. & Feller, M. B. (2011). Transgenic mice reveal unexpected diversity of on-off direction-selective retinal ganglion cell subtypes and brain structures involved in motion processing. *The Journal of Neuroscience*, *31*(24), 8760-8769.

Roberts, J. M., Ennajdaoui, H., Edmondson, C., Wirth, B., Sanford, J. R., & Chen, B. (2014). Splicing factor TRA2B is required for neural progenitor survival. *Journal of Comparative Neurology*, *522*(2), 372-392.

Rossi, F. M., Pizzorusso, T., Porciatti, V., Marubio, L. M., Maffei, L., & Changeux, J. P. (2001). Requirement of the nicotinic acetylcholine receptor β2 subunit for the anatomical and functional development of the visual system. *Proceedings of the National Academy of Sciences*, *98*(11), 6453-6458.

Sanes, J. R., & Masland, R. H. (2015). The types of retinal ganglion cells: current status and implications for neuronal classification. *Annual review of neuroscience*, (0).

Saper, C. B., Scammell, T. E., & Lu, J. (2005). Hypothalamic regulation of sleep and circadian rhythms. *Nature*, *437*(7063), 1257-1263.

Schiller, P. H., Stryker, M., Cynader, M., & Berman, N. (1974). Response characteristics of single cells in the monkey superior colliculus following ablation or cooling of visual cortex. *J. neurophysiol*, *37*, 181-194.

Schmidt, M., Zhang, H. Y., & Hoffmann, K. P. (1993). OKN-related neurons in the rat nucleus of the optic tract and dorsal terminal nucleus of the accessory optic system receive a direct cortical input. *Journal of Comparative Neurology*, *330*(2), 147-157.

Schmidt, T. M., Chen, S. K., & Hattar, S. (2011). Intrinsically photosensitive retinal ganglion cells: many subtypes, diverse functions. *Trends in neurosciences*, *34*(11), 572-580.

Schmitzer-Torbert, N., Jackson, J., Henze, D., Harris, K., & Redish, A. D. (2005). Quantitative measures of cluster quality for use in extracellular recordings. *Neuroscience*, *131*(1), 1-11.

Seabrook, T. A., El-Danaf, R. N., Krahe, T. E., Fox, M. A., & Guido, W. (2013). Retinal input regulates the timing of corticogeniculate innervation. *The Journal of Neuroscience*, *33*(24), 10085-10097.

Shang, C., Liu, Z., Chen, Z., Shi, Y., Wang, Q., Liu, S., Dapeng, L. & Cao, P. (2015). A parvalbumin-positive excitatory visual pathway to trigger fear responses in mice. *Science*, *348*(6242), 1472-1477.

Sillito, A. M., Cudeiro, J., & Jones, H. E. (2006). Always returning: feedback and sensory processing in visual cortex and thalamus. *Trends in neurosciences*, *29*(6), 307-316.

Sperry, R. W. (1963). Chemoaffinity in the orderly growth of nerve fiber patterns and connections. *Proceedings of the National Academy of Sciences of the United States of America*, *50*(4), 703.

Sretavan, D. W., Shatz, C. J., & Stryker, M. P. (1988). Modification of retinal ganglion cell axon morphology by prenatal infusion of tetrodotoxin. *Nature*, *336*(6198), 468-471.

Stoerig, P., & Cowey, A. (1997). Blindsight in man and monkey. *Brain*, *120*(3), 535-559

Su, J., Haner, C. V., Imbery, T. E., Brooks, J. M., Morhardt, D. R., Gorse, K., Guido, W. & Fox, M. A. (2011). Reelin is required for class-specific retinogeniculate targeting. *The Journal of Neuroscience*, *31*(2), 575-586.

Sun, L. O., Brady, C. M., Cahill, H., Al-Khindi, T., Sakuta, H., Dhande, O. S., Noda, M., Huberman, A.D., Nathans, J. & Kolodkin, A. L. (2015). Functional assembly of accessory optic system circuitry critical for compensatory eye movements. *Neuron*, *86*(4), 971-984.

Sweeney, N. T., Tierney, H., & Feldheim, D. A. (2014). Tbr2 is required to generate a neural circuit mediating the pupillary light reflex. *The Journal of Neuroscience*, *34*(16), 5447-5453.

Theyel, B. B., Llano, D. A., & Sherman, S. M. (2010). The corticothalamocortical circuit drives higher-order cortex in the mouse. *Nature neuroscience*, *13*(1), 84-88.

Trejo, L. J., & Cicerone, C. M. (1984). Cells in the pretectal olivary nucleus are in the pathway for the direct light reflex of the pupil in the rat. *Brain research*, *300*(1), 49-62.

Triplett, J. W., Wei, W., Gonzalez, C., Sweeney, N. T., Huberman, A. D., Feller, M. B., & Feldheim, D. A. (2014). Dendritic and axonal targeting patterns of a genetically-specified class of retinal ganglion cells that participate in image-forming circuits. *Neural Dev*, *9*(1), 2.

Tye, C., & Bolton, P. (2013). Neural connectivity abnormalities in autism: Insights from the Tuberous Sclerosis model. *BMC medicine*, *11*(1), 55.

Van Battum, E. Y., Brignani, S., & Pasterkamp, R. J. (2015). Axon guidance proteins in neurological disorders. *The Lancet Neurology*, *14*(5), 532-546.

Vorhees, C. V., & Williams, M. T. (2006). Morris water maze: procedures for assessing spatial and related forms of learning and memory. *Nature protocols*, *1*(2), 848-858.

Wang, L., Sarnaik, R., Rangarajan, K., Liu, X., & Cang, J. (2010). Visual receptive field properties of neurons in the superficial superior colliculus of the mouse. *The Journal of Neuroscience*, *30*(49), 16573-16584.

Wang, Q., & Burkhalter, A. (2013). Stream-related preferences of inputs to the superior colliculus from areas of dorsal and ventral streams of mouse visual cortex. *The Journal of neuroscience*, *33*(4), 1696-1705.

Wässle, H. (2004). Parallel processing in the mammalian retina. *Nature Reviews Neuroscience*, *5*(10), 747-757.

Williams, R. W., & Herrup, K. (1988). The control of neuron number. *Annual review of neuroscience*, *11*(1), 423-453.

Wiltschko, A. B., Gage, G. J., & Berke, J. D. (2008). Wavelet filtering before spike detection preserves waveform shape and enhances single-unit discrimination. *Journal of neuroscience methods*, *173*(1), 34-40.

Zhao, X., Liu, M., & Cang, J. (2014). Visual cortex modulates the magnitude but not the selectivity of looming-evoked responses in the superior colliculus of awake mice. *Neuron*, *84*(1), 202-213.